NACA

RESEARCH MEMORANDUM

LOW-SPEED WIND-TUNNEL INVESTIGATION OF A THIN 60° DELTA WING WITH DOUBLE SLOTTED, SINGLE SLOTTED, PLAIN, AND SPLIT FLAPS

By John M. Riebe and Richard G. MacLeod

Langley Aeronautical Laboratory
Langley Field, Va.

NATIONAL ADVISORY COMMITTEE
FOR AERONAUTICS

WASHINGTON

January 6, 1953
Declassified November 14, 1956

NATIONAL ADVISORY COMMITTEE FOR AERONAUTICS

RESEARCH MEMORANDUM

LOW-SPEED WIND-TUNNEL INVESTIGATION OF A THIN 60° DELTA WING WITH DOUBLE SLOTTED, SINGLE SLOTTED, PLAIN, AND SPLIT FLAPS

By John M. Riebe and Richard G. MacLeod

SUMMARY

A low-speed wind-tunnel investigation was made to determine the longitudinal aerodynamic characteristics of a thin delta wing equipped with various arrangements of double slotted, single slotted, plain, and split flaps. The wing was a flat plate with beveled leading and trailing edges and had a maximum thickness ratio of 0.045, and 60° sweepback of the leading edge.

The optimum double-slotted-flap arrangement tested resulted in an increment in lift coefficient of 0.96 at 0° angle of attack and an increase in the maximum lift coefficient of 0.36. The angle of attack required to obtain a given lift coefficient was considerably reduced with deflection of the double slotted flaps. For lift coefficients above 0.8, the lift-drag ratio for the wing with double slotted flaps deflected was higher than that of the plain wing.

The maximum increments of lift at zero angle of attack for the single slotted, plain, and split flaps were almost equal (lift coefficient approximately 0.45) and relatively low compared with the increment for the double slotted flaps. The single slotted flap produced some increment in maximum lift coefficient (0.24) but the increment for the plain and split flap was small. Lift-effectiveness estimates made from two-dimensional investigations and plain-flap theory agreed with the experimental lift effectiveness of the split and double slotted flap at low angles of attack.

INTRODUCTION

At the present time, there is considerable interest in the use of delta-wing plan forms for high-speed airplanes. This plan form exhibits

desirable aerodynamic characteristics at transonic and low-supersonic speeds and possesses advantageous structural characteristics. At low speeds the longitudinal stability problem appears to be less severe for delta wings than for conventional sweptback wings. However, the delta wing requires an undesirably high landing attitude to obtain high lift coefficients. The problem of attaining low landing speeds is therefore not only one of increasing the maximum lift coefficient but also, and frequently this is the more important consideration, one of decreasing the angle of attack required to achieve a given lift coefficient.

Investigations are currently being made in the Langley 300 MPH 7- by 10-foot tunnel to determine the effect of various trailing-edge high-lift devices on thin delta wings in an attempt to improve the landing characteristics. An exploratory investigation (ref. 1) showed the practicability of using double slotted flaps on delta wings.

The present investigation is an extension of the investigation reported in reference 1 but encompasses a more detailed study of the effect of vane and flap position and deflection, as well as the effect of small modifications, such as fairing the lower wing lip, on the aerodynamic characteristics of a delta wing. Also included are some studies of single slotted, plain, and split flaps. Particular attention was directed to the gain in lift coefficient that could be obtained in the low angle-of-attack range.

COEFFICIENTS AND SYMBOLS

The results of the tests are presented as standard NACA coefficients of forces and moments about the stability axes. Pitching-moment coefficients are given about the wing 25-percent-mean-aerodynamic-chord point shown in figure 1. The positive directions of forces, moments, angles, and distances are shown in figures 2 and 3.

The coefficients and symbols are defined as follows:

C_L lift coefficient, $\frac{L}{qS}$

C_D drag coefficient, $\frac{D}{qS}$

C_m pitching-moment coefficient, $\frac{M}{qS\bar{c}}$

L lift, lb

D	drag, lb
M	pitching moment, ft-lb
q	free-stream dynamic pressure, lb/sq ft, $\frac{1}{2}\rho V^2$
S	wing area, 6.93 sq ft
$\bar{c}$	wing mean aerodynamic chord, 2.31 ft, $\frac{2}{S}\int_0^{b/2} c^2 dy$
b	wing span, 4.00 ft
V	free-stream velocity, ft/sec
ρ	mass density of air, slugs/cu ft
δ_f	flap deflection measured in a plane perpendicular to hinge line, deg
δ_v	vane deflection measured in a plane perpendicular to hinge line, deg
α	angle of attack of wing, deg
c	local wing chord, ft
t	local wing thickness, ft
y	lateral distance from plane of symmetry, measured parallel to Y-axis, ft
x_f	horizontal distance of flap leading edge (station 0, table II) from wing-upper-surface lip, in.
x_v	horizontal distance of vane leading edge (station 0, table III) from wing-upper-surface lip, in.
z_f	vertical distance of flap leading edge (station 0, table II) from wing-upper-surface lip, in.
z_v	vertical distance of vane leading edge (station 0, table III) from wing-upper-surface lip, in.

MODEL AND APPARATUS

The model was tested in the Langley 300 MPH 7- by 10-foot tunnel by utilizing a sting-support system (fig. 4) and an electrical strain-gage balance.

The wing of the model had a 60° apex angle (aspect ratio 2.31) and a taper ratio of 0 (fig. 1 and table I). The model was made from a flat steel plate 5/8 inch thick, with beveled leading and trailing edges. The thickness ratio varied from 0.015c at the root to a maximum of 0.045c at 0.67 $\frac{b}{2}$. A flat airfoil was used because of the simple construction involved. A small fuselage was used to house the electrical strain-gage balance (figs. 1 and 4) and does not necessarily represent a typical fuselage.

Drawings of the four flap configurations used in this investigation are presented in figure 3. The slotted flap consisted of a brass leading edge (table II) attached to a steel wedge. A vane constructed of steel to the ordinates given in table III was attached to the slotted flap to make the double slotted flap. The plain-flap configuration was obtained by deflecting the single slotted flap about a point near its leading edge and filling the flap upper surface with modeling clay to attain a smooth curve from the wing to the flap trailing edge (fig. 3). The constant chord split flap used in this investigation was made of 1/8 sheet aluminum with the same chord as the flap part of the double slotted flap.

TESTS

The tests were made at a dynamic pressure of approximately 25 pounds per square foot, corresponding to an airspeed of about 100 miles an hour. Reynolds number for this airspeed based on the mean aerodynamic chord (2.31 ft), was approximately 2.2×10^6. The corresponding Mach number was 0.13. The tests were run through an angle-of-attack range of -20° to 42°.

CORRECTIONS

Jet-boundary corrections have been applied to the angles of attack and the drag coefficients. The corrections obtained from methods similar to those outlined in reference 2, were as follows:

$$\Delta\alpha = 1.70\ C_L\ (\text{deg})$$

$$\Delta C_D = 0.0297\ C_L^2$$

A correction has been applied to the angle of attack to account for the deflection of the support sting under load. No correction has been applied to the data for blocking because it was found to be negligible.

RESULTS AND DISCUSSION

Determination of Optimum Double-Slotted-Flap Arrangements

In order to obtain an indication of the vane-flap arrangement required for the highest lift increments, the vane was secured with respect to the wing in three different positions (which were chosen after consideration of ref. 1 and some unpublished data). Force data were obtained with the flap deflected 45° at various horizontal and vertical positions. Figure 5 presents the lift, drag, and pitching-moment characteristics for this series of tests. The physical dimensions for each position, which is numbered for reference purposes, are also included in this figure. The lift-coefficient results are summarized and presented in figure 6 as contours of lift coefficient for various positions of the flap nose. As was found in the results of another double-slotted-flap configuration (ref. 1), the double slotted flap with vane positions 1 and 2 had good effectiveness in producing lift. With the flap located in an optimum position, there was little difference in lift effectiveness between vane positions 1 and 2; however, as the gap between the vane and wing upper lip was increased to position 3, the lift effectiveness was reduced considerably (fig. 6).

For high angles of attack below the stall, the delta wing for vane positions 1 and 2 was generally neutrally stable longitudinally, but with the vane in position 3 was generally stable throughout the entire angle-of-attack range tested (fig. 5(c)).

At a given lift coefficient above 0.8, the drag coefficients for the wing with vane positions 1 and 2 were less than that of the plain wing and, with the vane at position 3, were larger than that of the plain wing (fig. 5).

The effect of removing the lower lip of the wing, with the vane in position 2, is shown in figure 5(b). The flap position which had produced the largest increment in lift showed a further increase in C_L (lift-coefficient increment of 0.06 at $\alpha = 0^\circ$), a decrease in drag coefficient, and an increase in pitching-moment coefficient; however, when the vane-flap gap was increased, essentially no aerodynamic changes were noted when the lower wing lip was removed.

Aerodynamic Characteristics of Selected Double-Slotted-Flap Configurations

By using the data of figures 5 and 6 and of reference 1 as a guide, the vane was fixed with respect to the flap at five positions and tests were made with the vane-flap units at various deflections about a pivot point near the nose of the vane (fig. 7). The five units were tested with two pivot conditions: pivot point X (0.31 in. below and 0.28 in. behind the wing lip) and pivot Y (0.47 in. below and 0.28 in. behind the lip). Locations of the flap and vane at the various flap angles are given in table IV. Figure 8 presents the aerodynamic characteristics of each of the vane-flap units pivoted through a deflection range with the vane in position X (the smaller wing-lip vane gap). The data obtained by pivoting each of the vane flap units about point Y (the larger gap configuration) are shown in figure 9.

Lift coefficient.- Deflection of any of the vane-flap units on the delta wing resulted in large increments of lift coefficient throughout the angle-of-attack range (figs. 8 and 9). The increments were largest in the angle-of-attack range between 0° and 10° and became smaller as the stall angle of attack was approached. The largest lift coefficients at angles of attack of 0° and 10° were obtained for vane-flap unit E pivoted about point X (fig. 10(a)). When the double slotted flap was deflected 59°, the wing with vane position E had lift coefficients of 0.96 and 1.38 at angles of attack of 0° and 10°, respectively, and a maximum lift coefficient of 1.67. This compares to lift-coefficient values of 0, 0.46, and 1.40 for the plain wing at the same angles of attack and maximum lift condition. However, several vane-flap units, at high deflection angles, (figs. 8 and 9) had some nonlinearity in the lift-coefficient curves at high lift coefficients. A more nearly linear lift curve was usually obtained at lower flap deflections, however, with less lift increment at low angles of attack. The maximum lift coefficient for the wing with double slotted flaps occurred at an angle of attack about 5° less than that of the plain wing.

The angle of attack required to obtain a given lift coefficient for the delta wing was considerably reduced with deflection of the double slotted flaps. An angle of attack of about 21° was required for the plain wing to obtain a lift coefficient of 1.0, whereas an angle of attack of only about 1° was required to obtain the same lift coefficient for the wing with vane-flap unit E deflected 59° about pivot point X (fig. 8(e)). Use of the double slotted flap thus appears to offer a remedy to an important problem of the delta-wing airplane, decreasing the angle of attack required to achieve a given lift coefficient.

In general, for a given flap deflection, (figs. 10(a) and 10(b)) higher lift coefficients resulted when the vane-flap unit was located

nearer to the upper lip of the wing (pivot point X). The flap lift effectiveness was also maintained to higher deflection angles for the configuration where the vane-flap unit was pivoted closer to the wing upper lip. Flap lift effectiveness also held to higher deflection angles when the lower lip of the wing was removed (fig. 10(b)).

Pitching-moment coefficient.- With the vane-flap unit at either of the pivot points, the pitching-moment curves of the wing were longitudinally stable at low angles of attack but generally were unstable at the higher angles of attack (figs. 8 and 9). The pitching-moment curves for the wing of reference 1 with double slotted flap deflected had a stable break at the stall. The only difference between the model configuration of reference 1 and that of the present investigation was the vane section; it is, therefore, thought that the longitudinal instability of the wing for some of the double-slotted-flap configurations of the present investigation might be removed by alteration of the vane size and shape.

Deflection of all the double-slotted-flap configurations produced a diving moment which would result in some loss of lift coefficient when trimming the model with a conventional tail. For example, for an airplane with the double slotted flap with vane flap unit E deflected 59° about pivot point X, and with a tail length of $2\bar{c}$, the reduction in lift coefficient to counteract the pitching-moment coefficient increment between the plain wing and the deflected flap condition would be approximately 0.16.

The use of a horizontal tail to trim out the diving moment resulting from flap deflection would be expected to have a considerable effect on the longitudinal stability of delta-wing airplanes because of the large variations of downwash distribution behind delta wings. No effort was therefore made in the present investigation to eliminate the longitudinal instability whenever it occurred, the primary concern being the development of configurations which produced high lift coefficients at low angles of attack.

Drag characteristics.- Beyond a lift coefficient of approximately 0.8, the drag coefficient for the wing with flaps deflected was less than that of the plain wing so that the lift-drag ratios up to the stall were higher. A comparison of results for the plain wing and those for an optimum flap condition with respect to lift (vane flap unit E deflected 59° about pivot point X) in figure 8(e) show an increase in lift-drag ratio from 2.15 to 3.04 at a lift coefficient of 1.2.

Effect of slot and lip modifications.- Figures 9(a) and 10(b) show that removing the lower lip resulted in some gain in lift coefficient by extending the usable flap-deflection range. Very little change in pitching-moment coefficient and drag coefficient occurred with removal of the lower lip. No further change was observed when the slot between

the wing and vane was faired with a wooden block (such as that shown for the single slotted flap in fig. 3). The importance of not allowing upward deflection of the lip is indicated in figure 11 which are data obtained from an investigation (ref. 3) of various spoiler arrangements on delta wings with double slotted flaps. Although very little change in the aerodynamic characteristics of the delta wing equipped with the double slotted flap was observed when the upper lip was deflected downward, a considerable loss of lift and an increase in drag and a decrease in stability resulted when the lip was deflected upward a small amount.

Aerodynamic Characteristics of Single Slotted, Plain, and Split Flaps

Figures 12, 13, and 14 present the results for the wing equipped with a single slotted flap, a plain flap, and a split flap, respectively. The maximum lift coefficient and the lift coefficient at angles of attack of 0° and 10° are plotted against flap deflection in figure 15 for the three flap configurations. The single slotted flap developed less lift throughout the angle-of-attack range and less drag in the low lift-coefficient range than the double slotted flap. Both flap configurations stalled at approximately the same angle of attack but the single slotted flap had a stable break of the pitching-moment curve at the stall compared to an unstable break for some of the double-slotted-flap configurations. Generally there was very little difference between the aerodynamic characteristics of the plain flap and split flap.

Figure 15 indicates that in the range of flap deflections tested, the single slotted flap generally developed higher maximum lift, (increment from plain wing, 0.24) and produced it at a lower flap deflection, than either the plain or split flaps. In the lower angle-of-attack range, the single slotted, split, and plain flaps show relatively low flap effectiveness at high deflections (lift coefficient of approximately 0.45 at 0° angle of attack) as compared to the double slotted flaps of figure 10.

Estimated Flap Lift Effectiveness

Plain-flap effectiveness as determined from reference 4 is shown by the dashed line in figures 10 and 15. The curve represented in these figures is an extension to 50° of the plain-flap effectiveness computed in the 0° to 10° deflection range. Comparison of the estimated plain-flap effectiveness with the data for the double slotted flap suggests that the vane of the double slotted flap was essentially a boundary-layer-control device which held the plain-flap effectiveness to high deflection angles.

The diamond-shaped symbols in figures 10 and 15 are estimates of the lift increment at 0° angle of attack for the double slotted and split flaps, respectively, on the delta wing. These values were obtained by the combined use of reference 4 and split- and double-slotted-flap effectiveness, α/δ_f, of two-dimensional investigations and are in good agreement with the experimental data.

CONCLUSIONS

A low-speed wind-tunnel investigation of a thin delta wing equipped with various trailing-edge high-lift devices indicated the following:

1. The angle of attack required to obtain a given lift coefficient was considerably reduced with deflection of the double slotted flaps. A double-slotted-flap configuration resulted in an increment in lift coefficient of about 0.96 at 0° angle of attack and an increase in maximum lift coefficient of 0.36.

2. At lift coefficients above 0.8 the lift-drag ratio for the wing with double slotted flaps deflected was higher than that of the plain wing.

3. The maximum increments of lift at an angle of attack of 0° for a single slotted, plain, and a split flap were almost equal (lift coefficient approximately 0.45) and relatively low compared to the increment for the double slotted flap.

4. Lift-effectiveness estimates made from two-dimensional investigations and plain-flap theory, agreed with the experimental lift effectiveness of the split and double slotted flaps at low angles of attack.

Langley Aeronautical Laboratory,
National Advisory Committee for Aeronautics,
Langley Field, Va.

REFERENCES

1. MacLeod, Richard G.: A Preliminary Low-Speed Wind-Tunnel Investigation of a Thin Delta Wing Equipped With a Double and a Single Slotted Flap. NACA RM L51J26, 1952.

2. Gillis, Clarence L., Polhamus, Edward C., and Gray, Joseph L., Jr.: Charts for Determining Jet-Boundary Corrections for Complete Models in 7- by 10-Foot Closed Rectangular Wind Tunnels. NACA ARR L5G31, 1945.

3. Croom, Delwin R.: Characteristics of Flap-Type Spoiler Ailerons at Various Locations On a 60° Delta Wing With a Double Slotted Flap. NACA RM L52J24, 1952.

4. DeYoung, John: Theoretical Symmetric Span Loading Due to Flap Deflection for Wings of Arbitrary Plan Form at Subsonic Speeds. NACA TN 2278, 1951.

TABLE I

PHYSICAL CHARACTERISTICS OF THE TEST MODEL

Wing:	
Span, ft	4.00
Aspect ratio	2.31
Thickness of flat plate $\left(\left(\frac{t}{c}\right)_{max} = 0.045\right)$, in	5/8
Sweep, deg	60.00
Area, sq ft	6.93
Mean aerodynamic chord, ft	2.31
Leading-edge angle, deg	6.8
Taper ratio	0
Vane:	
Span, ft	2.70
Chord, ft	0.13
Chord, percent wing root chord	3.6
Chord, percent flap chord	27.3
Flap:	
Span, ft	2.70
Chord, ft	0.46
Chord, percent wing root chord	13.2
Area, sq ft	1.22
Area, percent wing area	17.6
Trailing-edge angle, deg	8.0

TABLE II

ORDINATES OF THE LEADING EDGE OF THE TRAILING-EDGE FLAP

[All dimensions in inches]

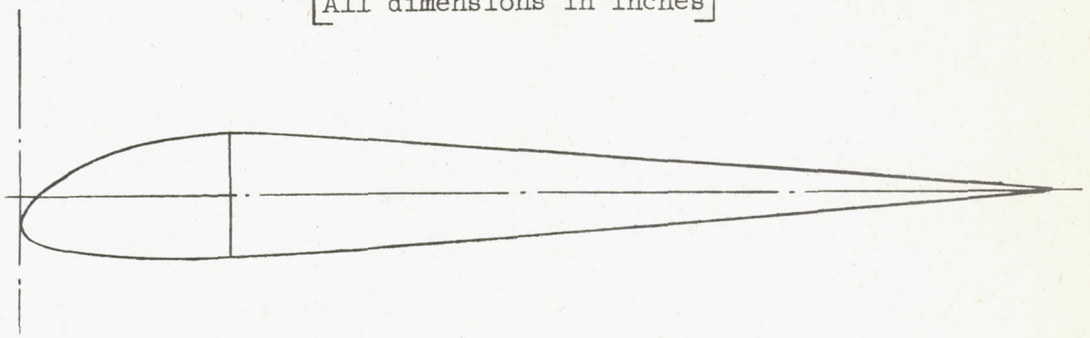

Station	Upper surface	Lower surface
0	-0.15	-0.15
.1	.01	-.25
.2	.08	-.27
.4	.18	-.29
.6	.25	-.30
.8	.30	-.31
1.1	.31	-.31

TABLE III

ORDINATES OF THE VANE

[All dimensions in inches]

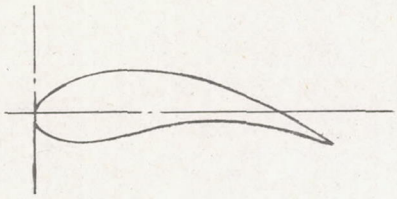

Station	Lower surface	Upper surface
0	0	0
.025	-.067	.051
.075	-.105	.100
.125	-.125	.130
.175	-.139	.153
.225	-.145	.175
.275	-.145	.190
.325	-.138	.205
.400	-.125	.219
.500	-.099	.221
.600	-.074	.215
.700	-.055	.205
.800	-.044	.180
.900	-.039	.153
1.000	-.042	.115
1.100	-.050	.075
1.200	-.066	.025
1.300	-.083	-.032
1.400	-.105	-.083
1.500	-.153	-.153

TABLE IV

LOCATION OF FLAP AND VANE FOR VARIOUS DOUBLE-SLOTTED-FLAP ARRANGEMENTS TESTED

Vane-flap unit	δ_f	x_f, in.	z_f, in.	δ_v	x_v, in.	z_v, in.	Data figure
Pivot point X							
A	49°00'	-1.32	0.50	-6°	0.06	0.37	8(a)
	53°35'	-1.30	.60	-2°	.06	.35	8(a)
	58°35'	-1.30	.68	4°	.06	.34	8(a)
	64°05'	-1.25	.76	14°	.06	.33	8(a)
	69°00'	-1.21	.83	14°	.06	.32	8(a)
B	44°50'	-1.23	.60	0°	.06	.36	8(b)
	49°50'	-1.20	.68	5°	.06	.34	8(b)
	55°30'	-1.19	.76	10°	.06	.32	8(b)
	60°00'	-1.13	.83	15°	.06	.30	8(b)
C	44°30'	-1.07	.82	9°	.06	.32	8(c)
	49°40'	-1.03	.90	14°	.06	.30	8(c)
	54°25'	-1.00	.95	19°	.06	.29	8(c)
	59°30'	-.94	1.20	24°	.06	.28	8(c)
D	53°40'	-1.23	1.12	11°	.06	.30	8(d)
	59°05'	-1.13	1.21	16°	.06	.29	8(d)
	63°20'	-1.05	1.28	21°	.06	.28	8(d)
E	48°35'	-1.10	1.25	19°	.06	.28	8(e)
	54°00'	-1.01	1.31	24°	.06	.27	8(e)
	59°00'	-.92	1.38	29°	.06	.26	8(e)
	64°00'	-.84	1.43	34°	.06	.24	8(e)
Pivot point Y							
A	44°00'	-1.37	0.56	-11°	0.06	0.51	9(a)
	53°45'	-1.30	.74	-1°	.06	.48	9(a)
	59°05'	-1.30	.82	4°	.06	.47	9(a)
	64°05'	-1.25	.90	9°	.06	.46	9(a)
	69°15'	-1.21	.97	14°	.06	.46	9(a)
B	45°25'	-1.23	.74	0°	.06	.48	9(b)
	50°15'	-1.20	.82	5°	.06	.47	9(b)
	56°10'	-1.19	.90	10°	.06	.46	9(b)
	60°40'	-1.13	.97	15°	.06	.45	9(b)
C	44°45'	-1.07	.96	9°	.06	.46	9(c)
	50°10'	-1.03	1.04	14°	.06	.44	9(c)
	55°00'	-1.00	1.09	19°	.06	.43	9(c)
D	49°15'	-1.33	1.19	11°	.06	.46	9(d)
	54°25'	-1.23	1.26	16°	.06	.45	9(d)
	59°25'	-1.13	1.35	21°	.06	.44	9(d)
E	44°00'	-1.20	1.31	13°	.06	.44	9(e)
	49°15'	-1.10	1.39	18°	.06	.42	9(e)
	54°00'	-1.01	1.45	23°	.06	.40	9(e)
	59°20'	-.92	1.52	28°	.06	.38	9(e)
	64°15'	-.84	1.57	33°	.06	.36	9(e)

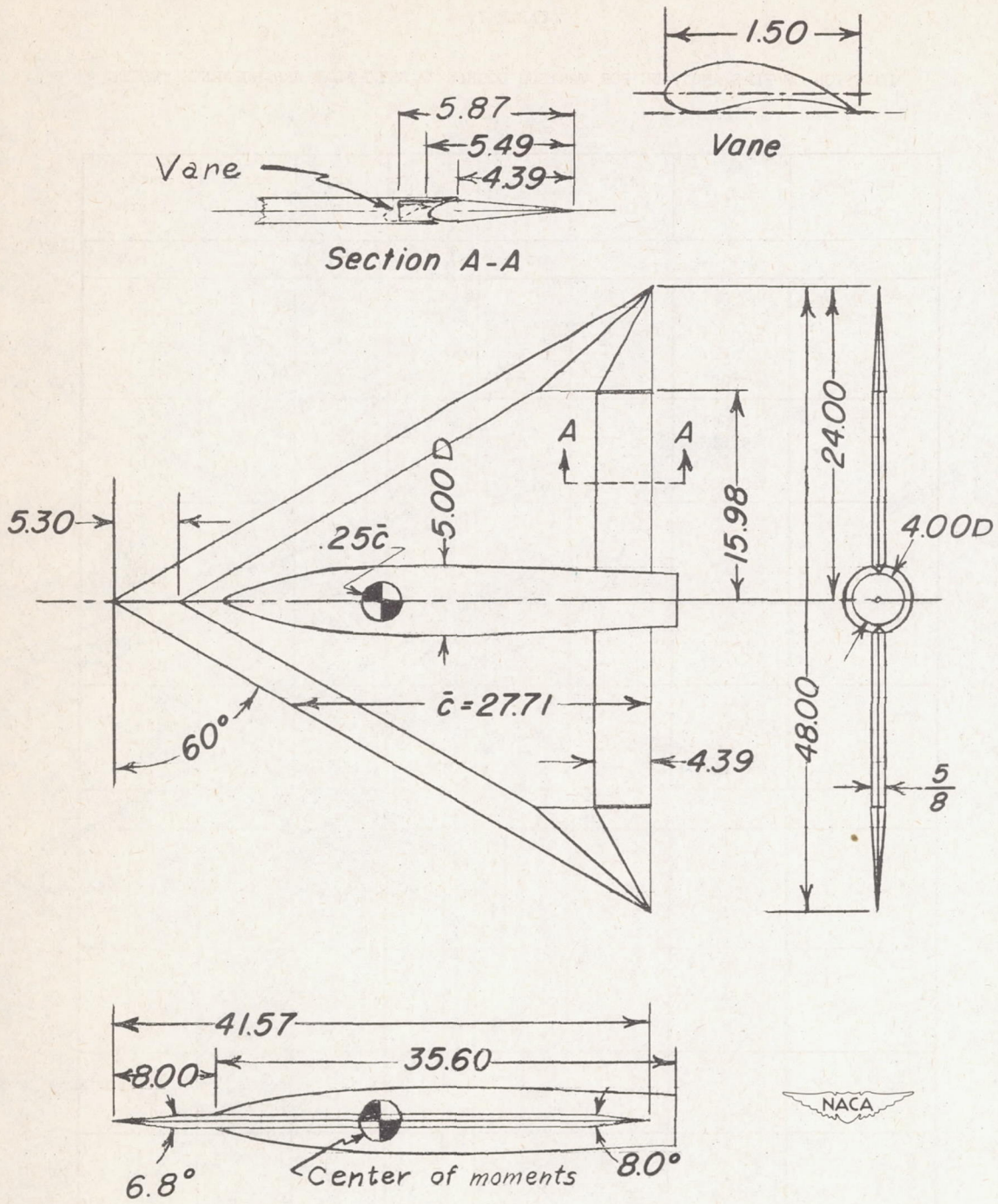

Figure 1.- General arrangement of the 60° delta-wing model. All dimensions are in inches.

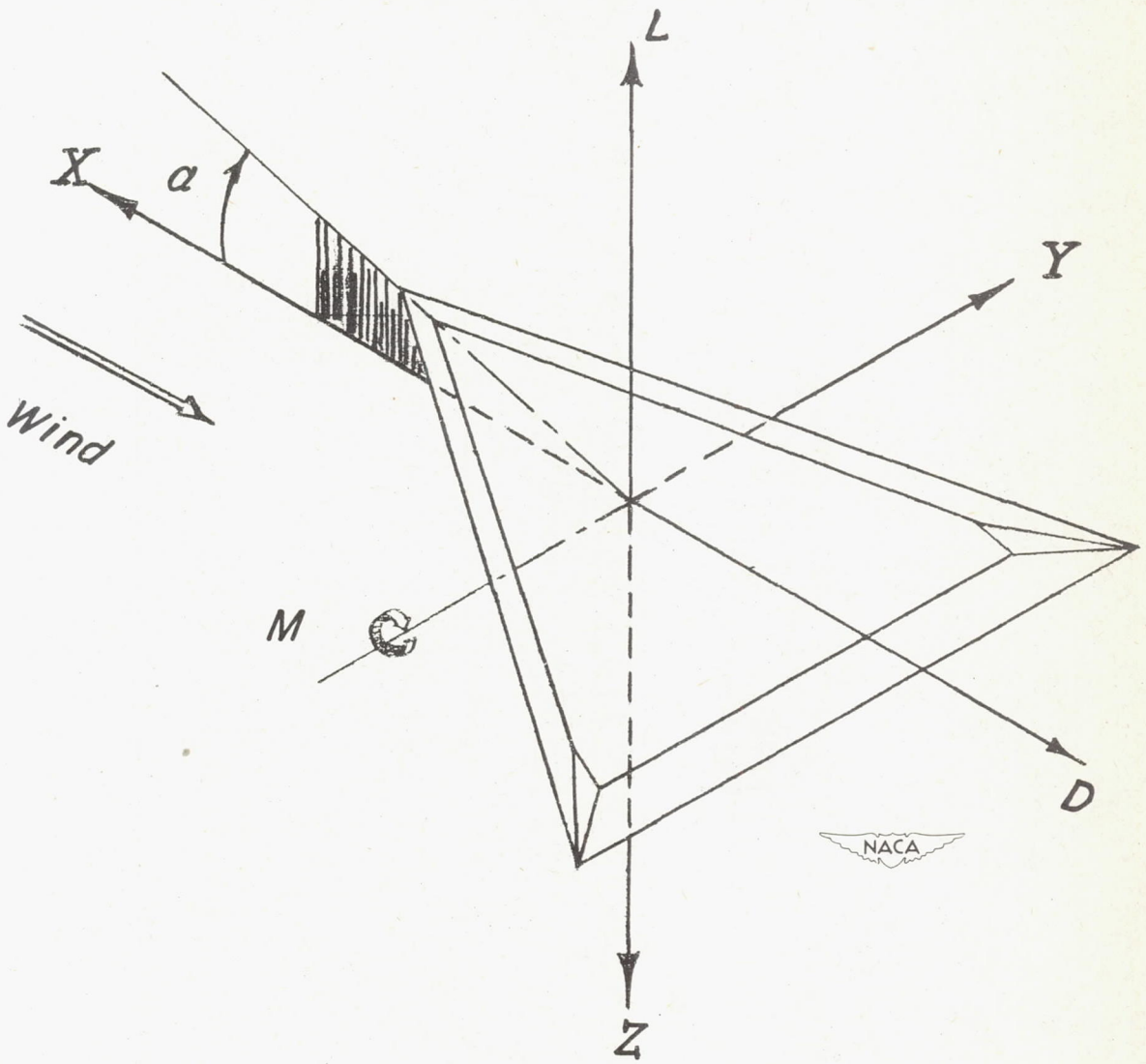

Figure 2.- System of stability axes. Positive values of forces, moments, angles, and distances are indicated by arrows.

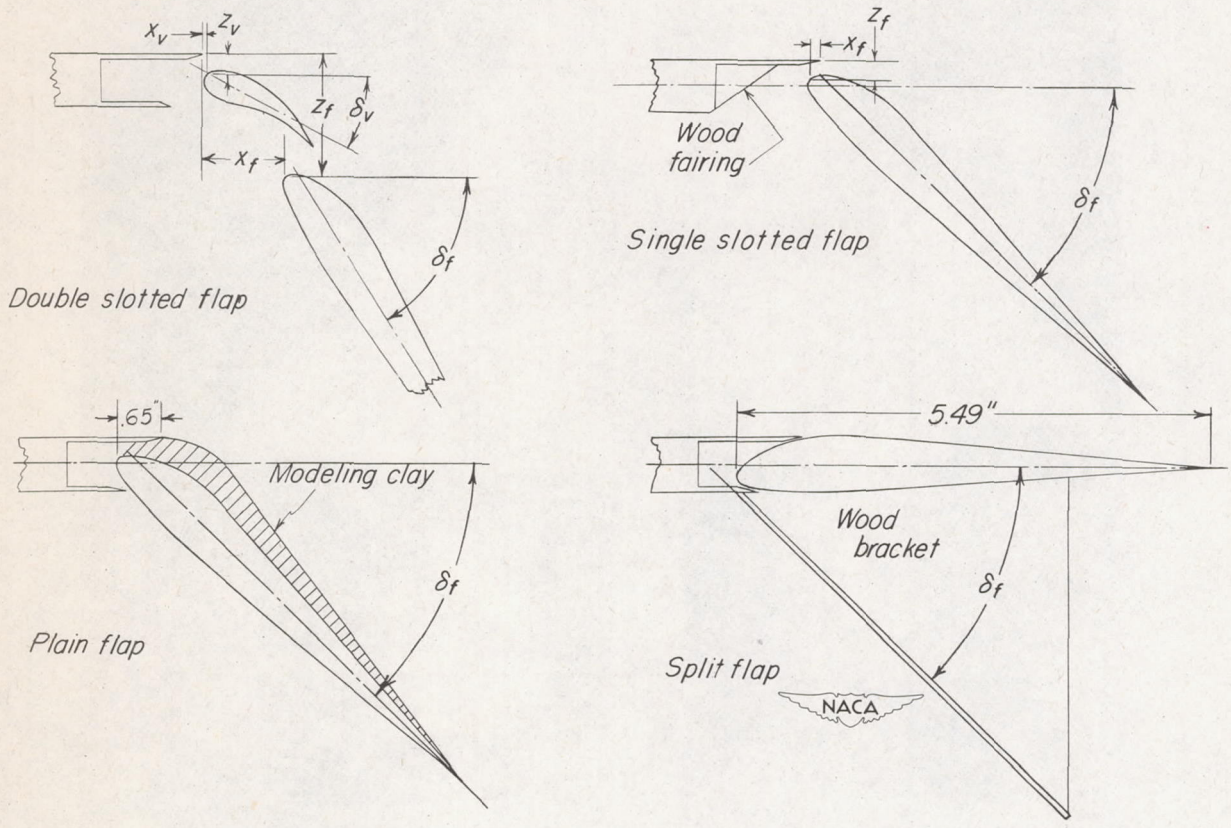

Note: The values of x measured from the wing upper lip are positive in the upstream direction and the values of z measured from the wing upper lip are positive in a direction toward the lower wing surface (similar to the positive directions for the stability axes, fig. 2).

Figure 3.- Double slotted, single slotted, plain, and split flaps tested on the 60° delta wing.

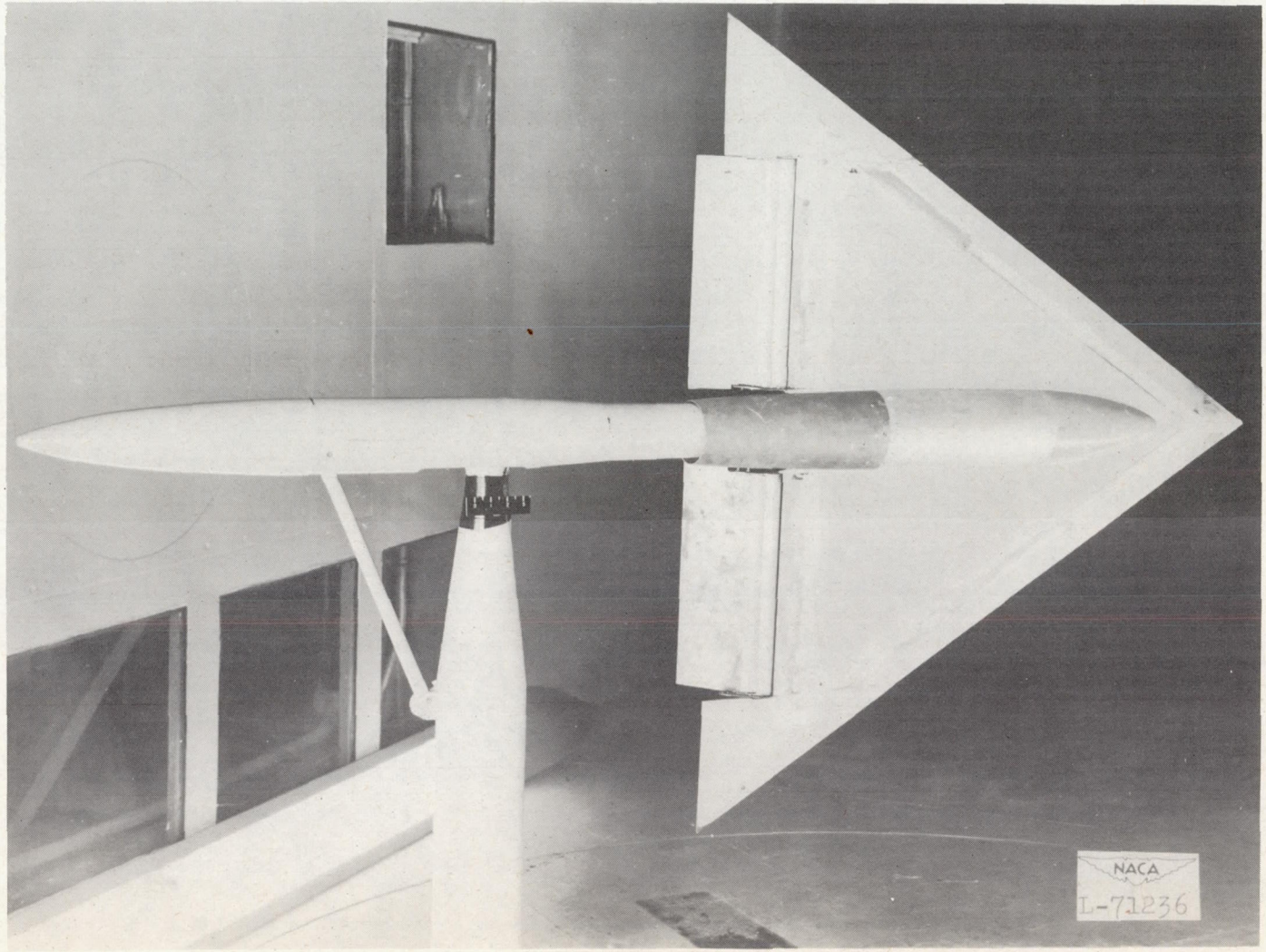

Figure 4.- The 60° delta wing mounted in the Langley 300 MPH 7- by 10-foot tunnel.

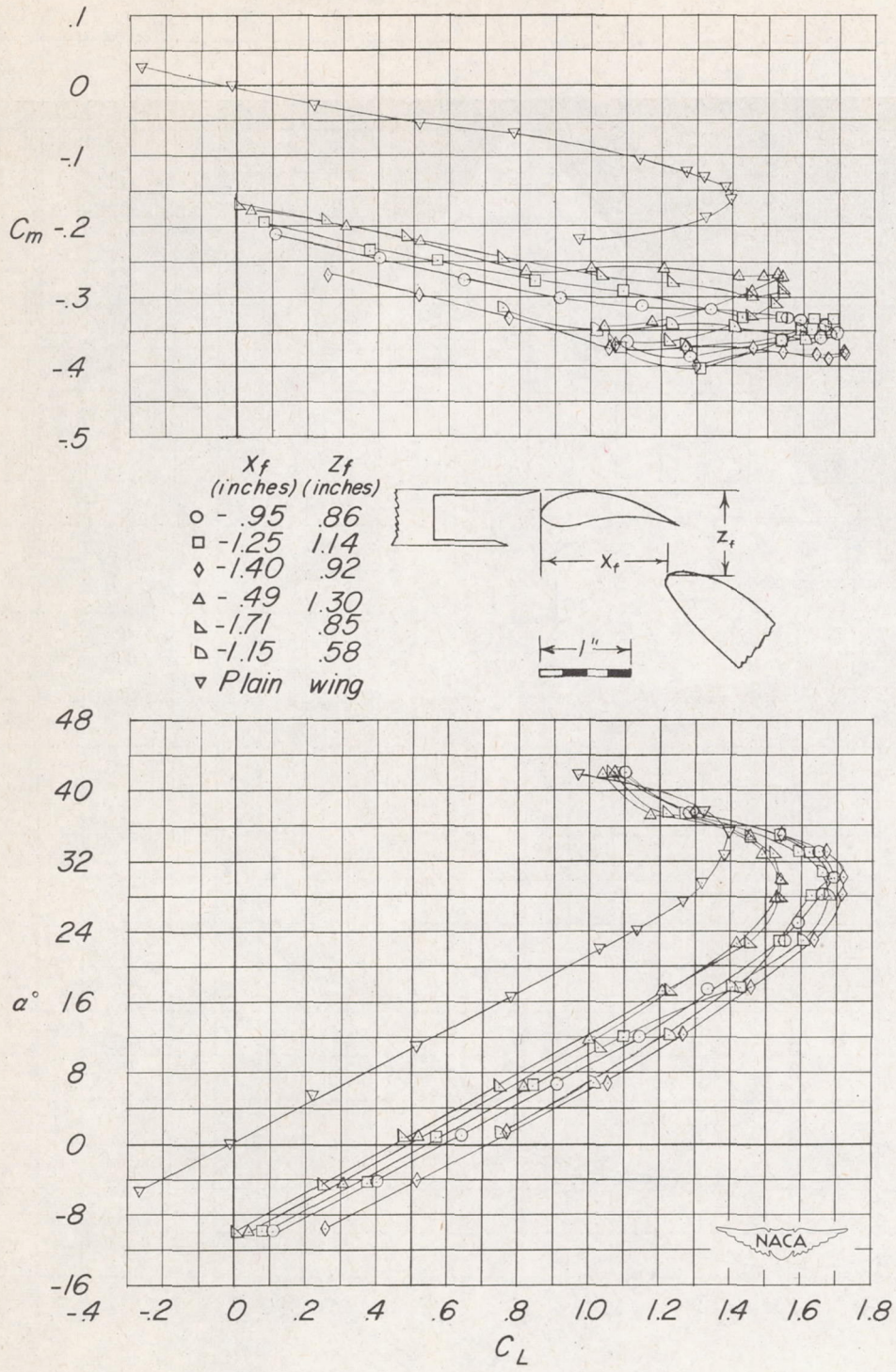

(a) Vane position 1: x_v = 0.0 inch; z_v = 0.26 inch; δ_v = 0°.

Figure 5.- The aerodynamic characteristics of the test model with a double slotted flap deflected 45°.

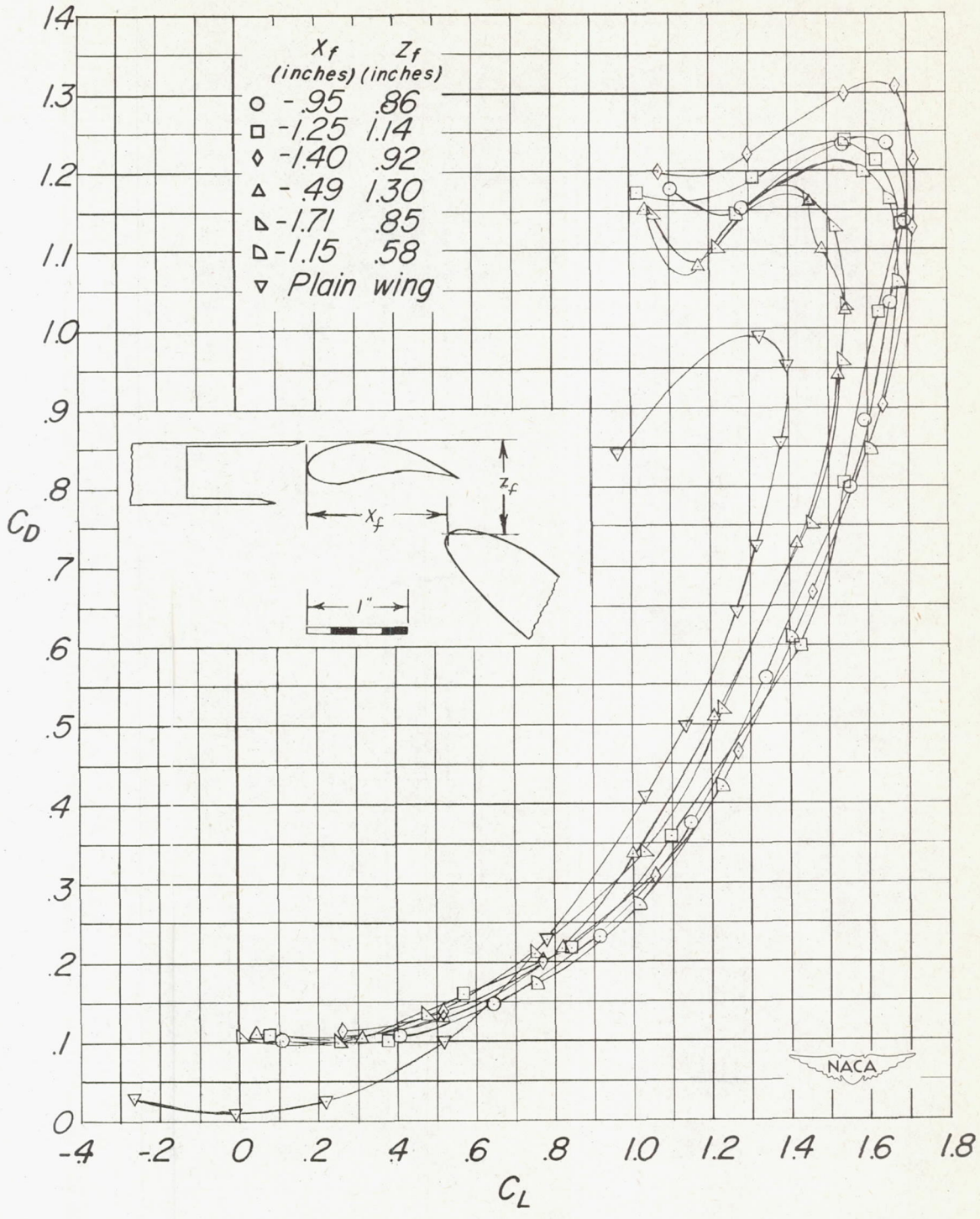

(a) Concluded.

Figure 5.- Continued.

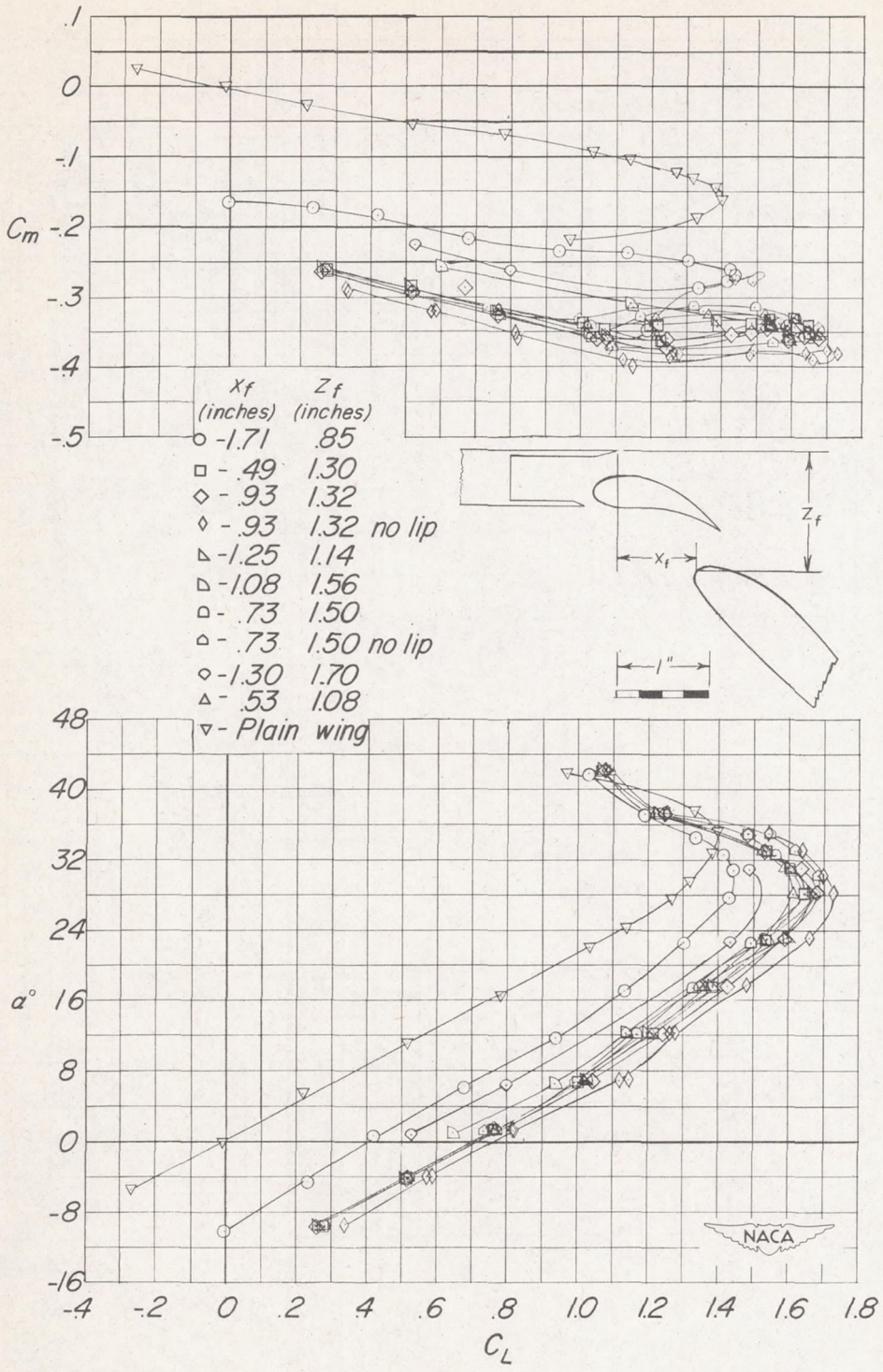

(b) Vane position 2: x_v = 0.23 inch; z_v = 0.40 inch; δ_v = 12.5°.

Figure 5.- Continued.

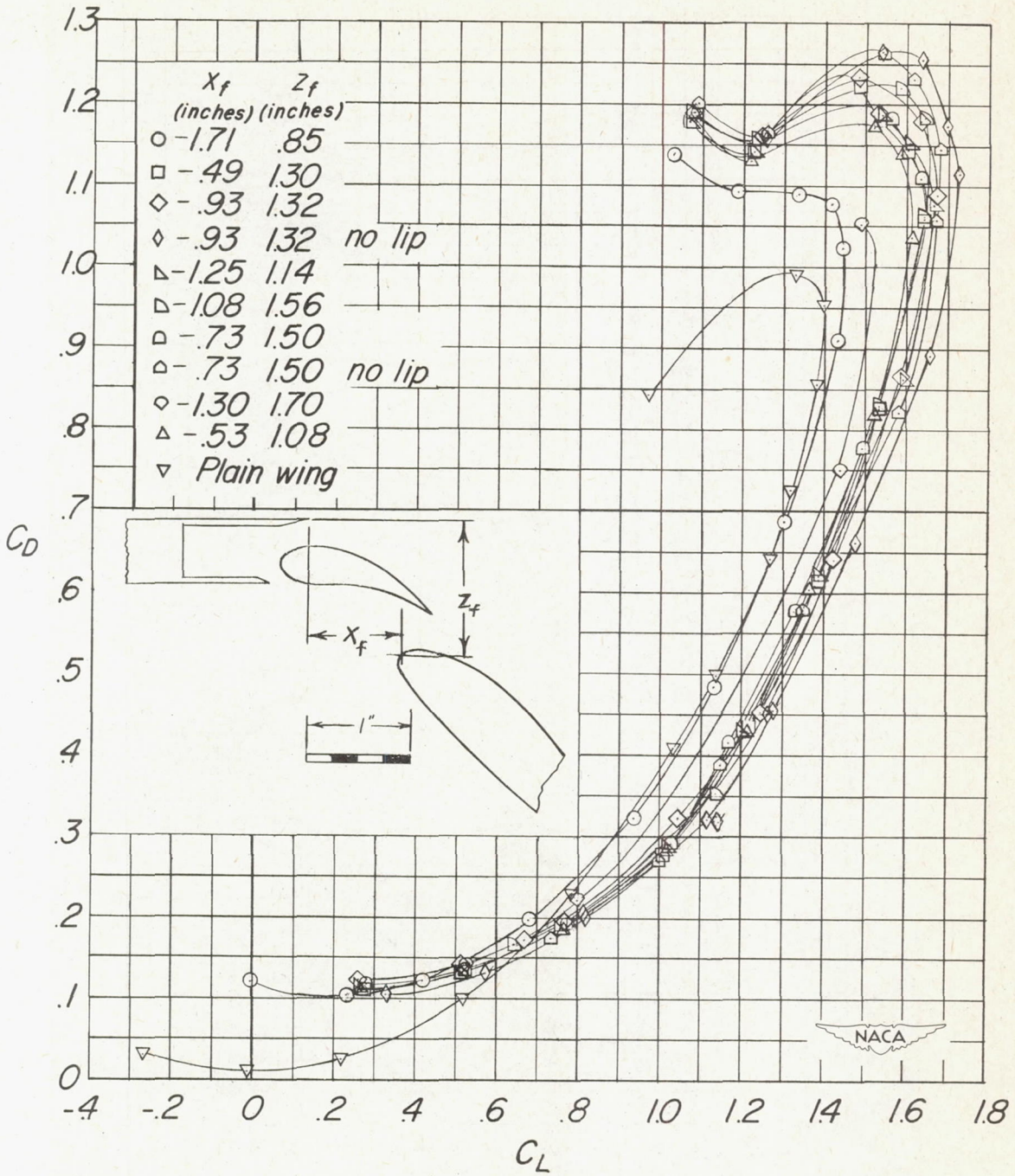

(b) Concluded.

Figure 5.- Continued.

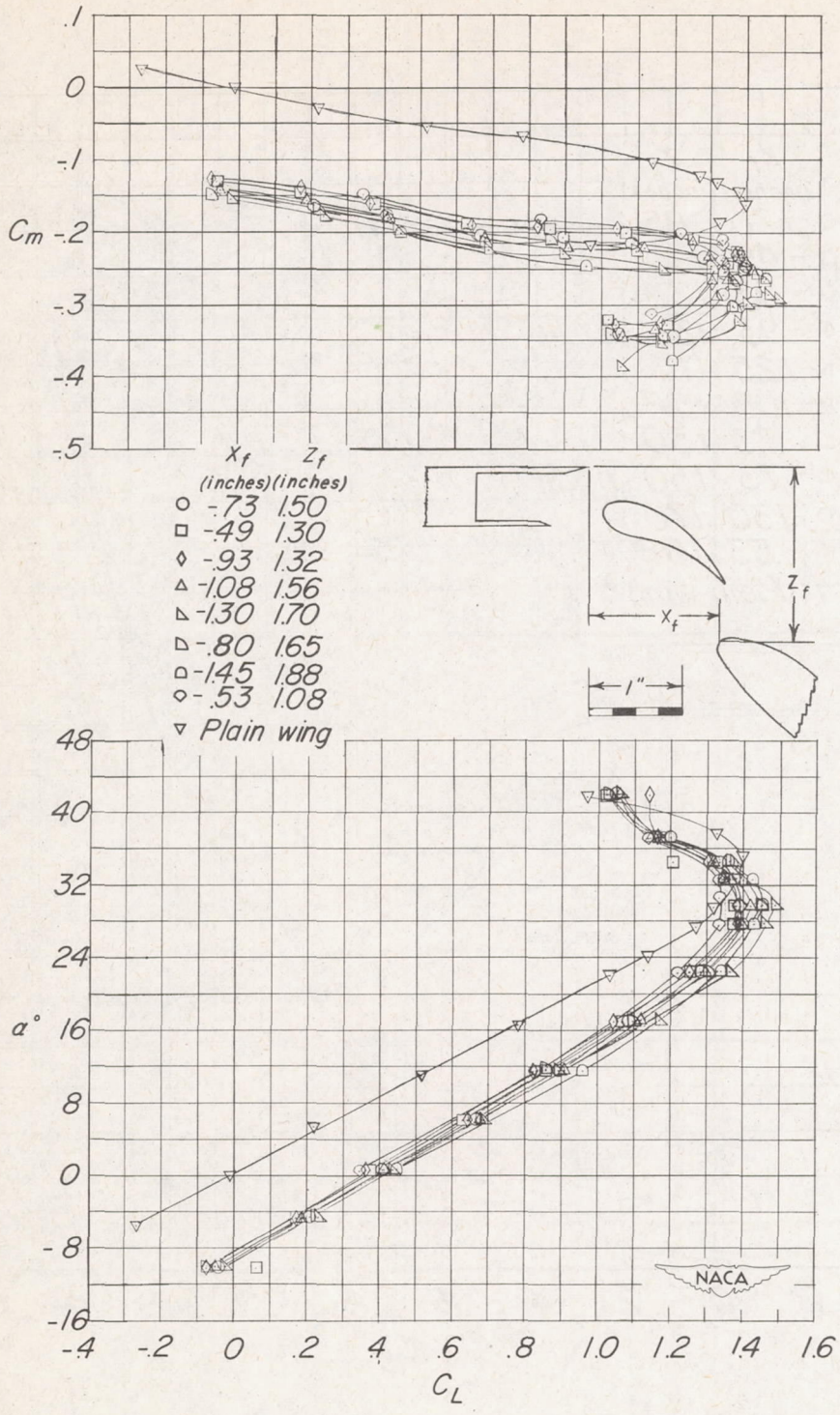

(c) Vane position 3: x_v = -0.20 inch; z_v = 0.42 inch; δ_v = 25.7°.

Figure 5.- Continued.

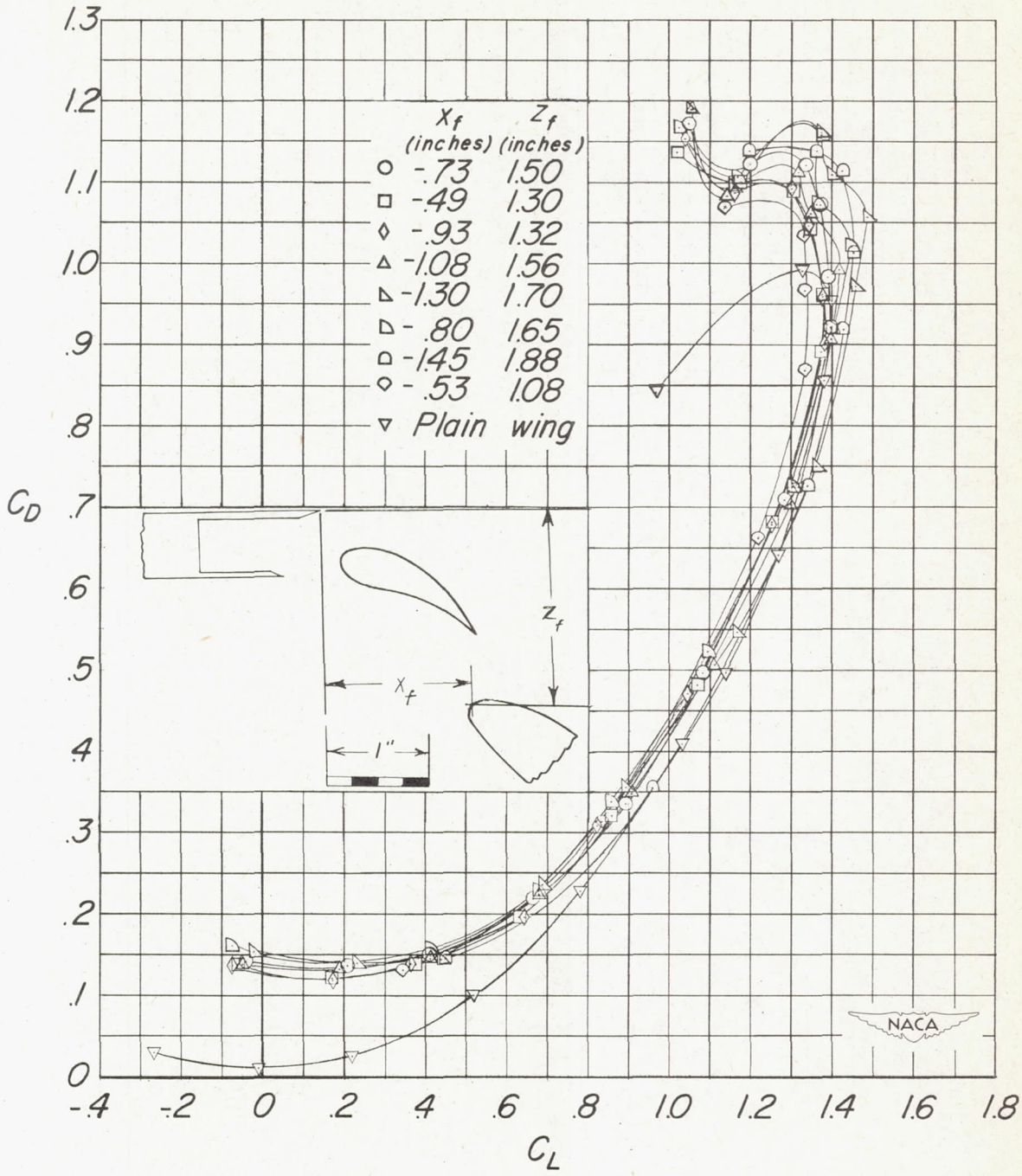

(c) Concluded.

Figure 5.- Concluded.

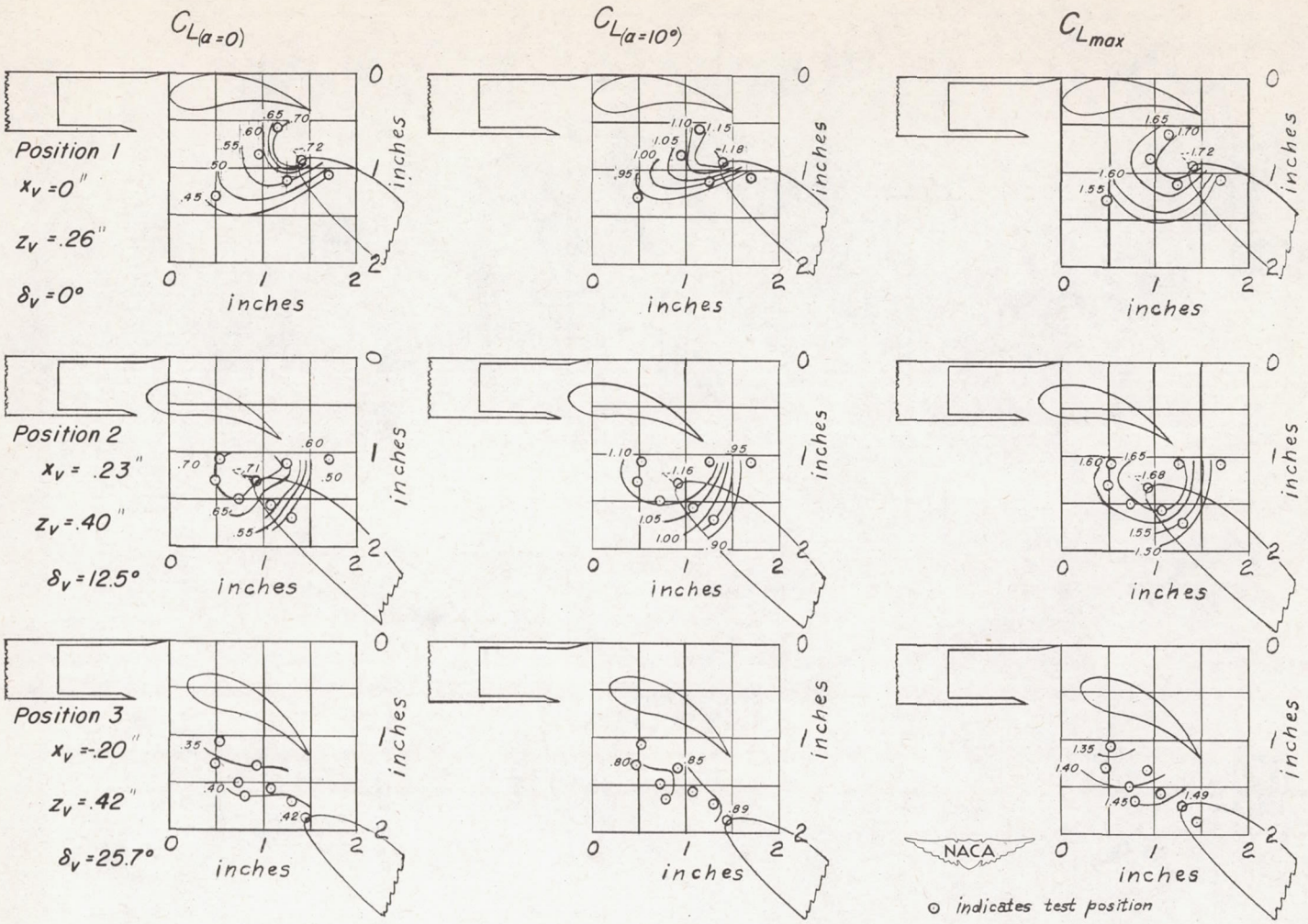

Figure 6.- Contours of lift coefficients for various flap nose positions for C_L at $\alpha = 0°$, C_L at $\alpha = 10°$, and $C_{L_{max}}$. $\delta_f = 45°$.

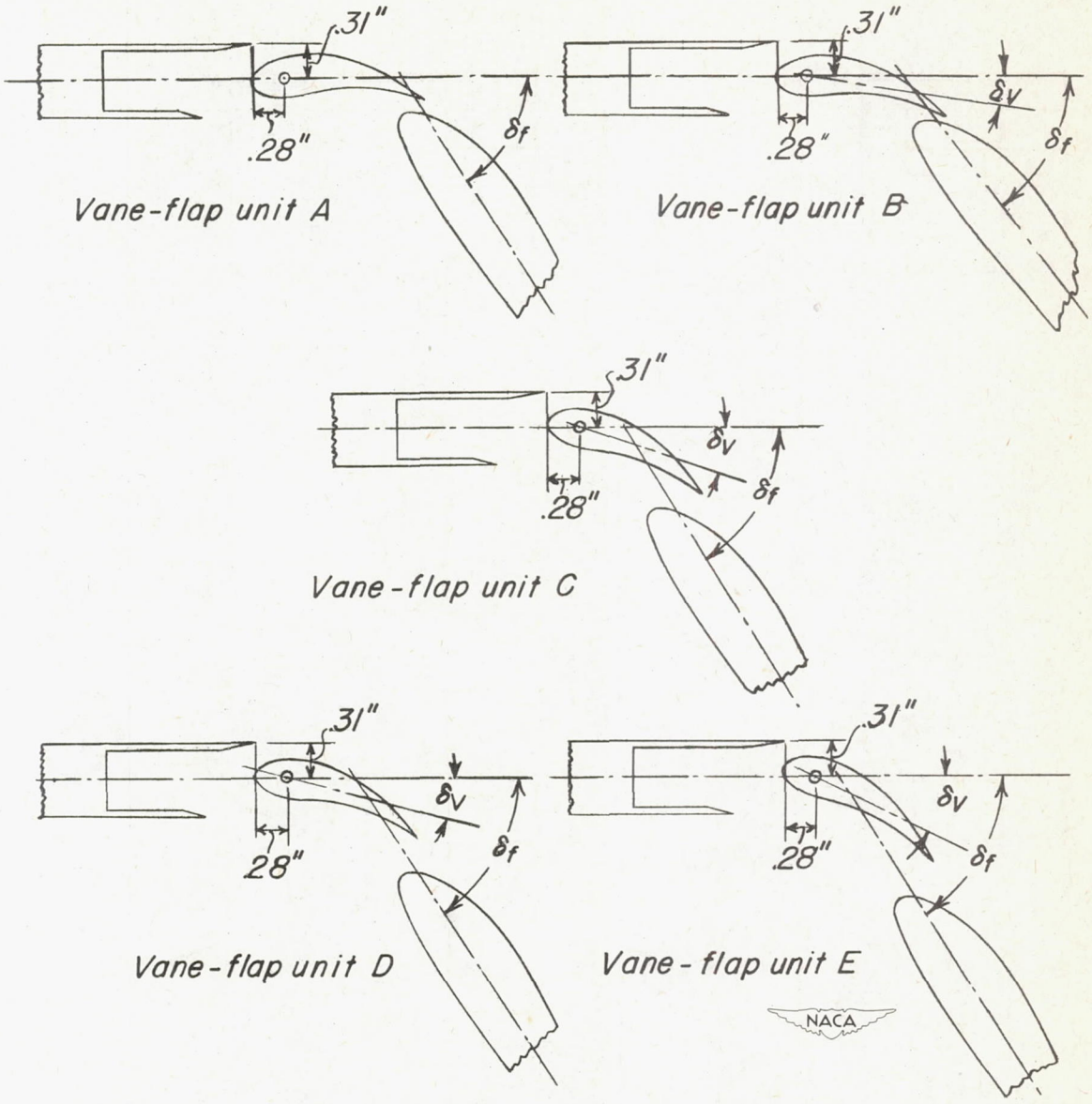

(a) Vane-flap unit pivoted about point X.

Figure 7.- Sectional view of the five vane-flap units tested on the model.

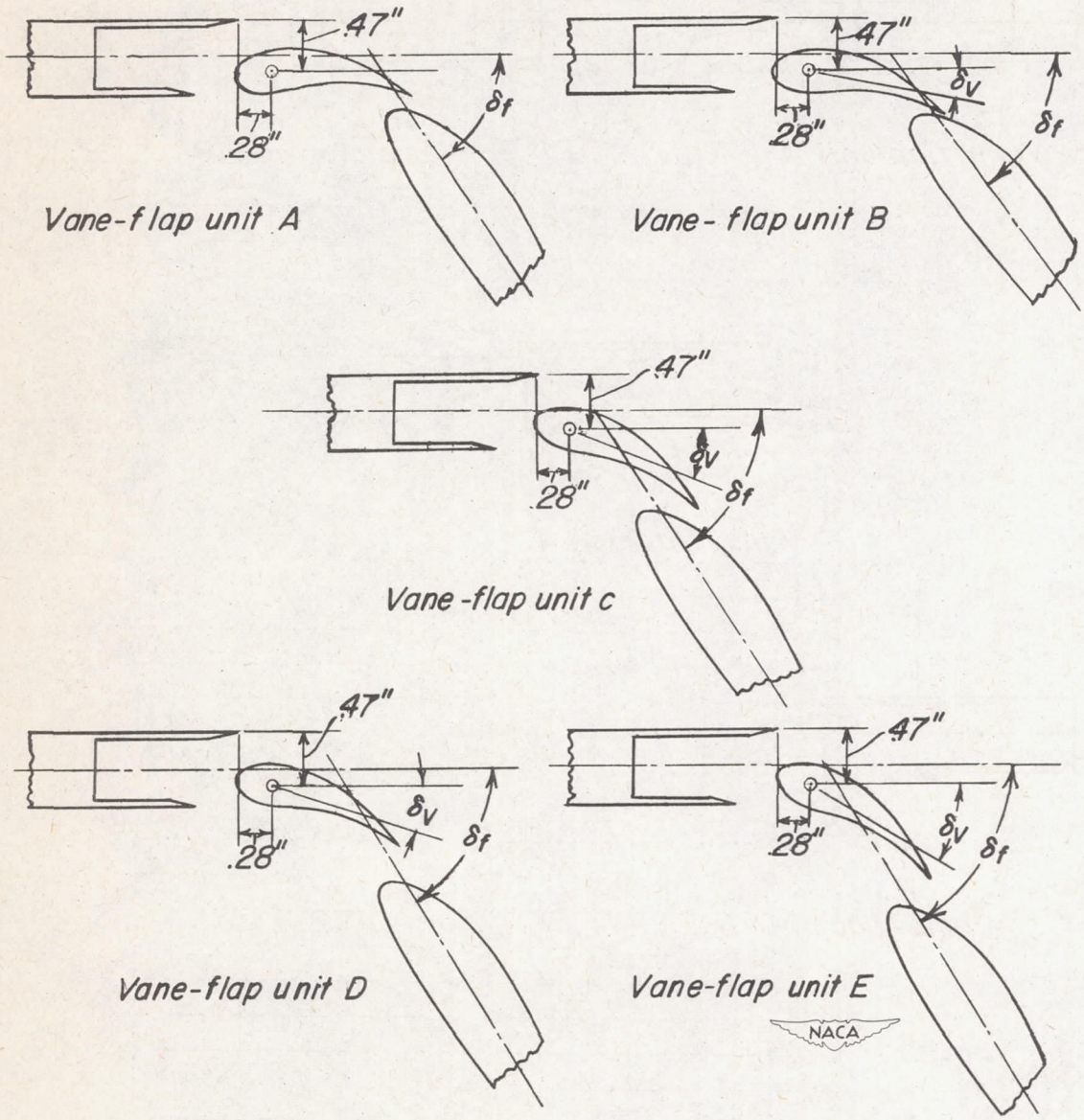

(b) Vane-flap unit pivoted about point Y.

Figure 7.- Concluded.

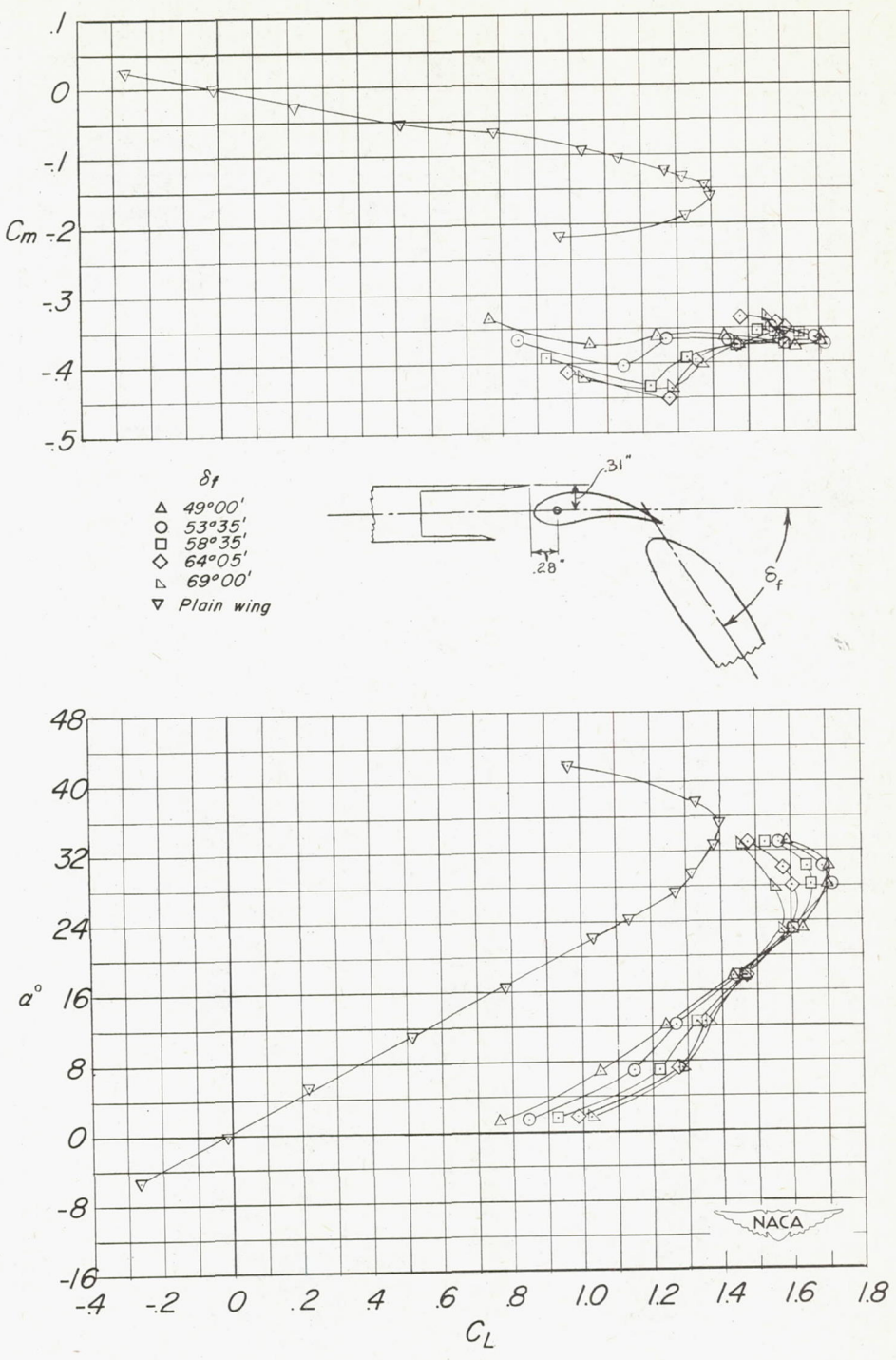

(a) Vane-flap unit A.

Figure 8.- The aerodynamic characteristics of the test model with the vane-flap unit pivoted about point X.

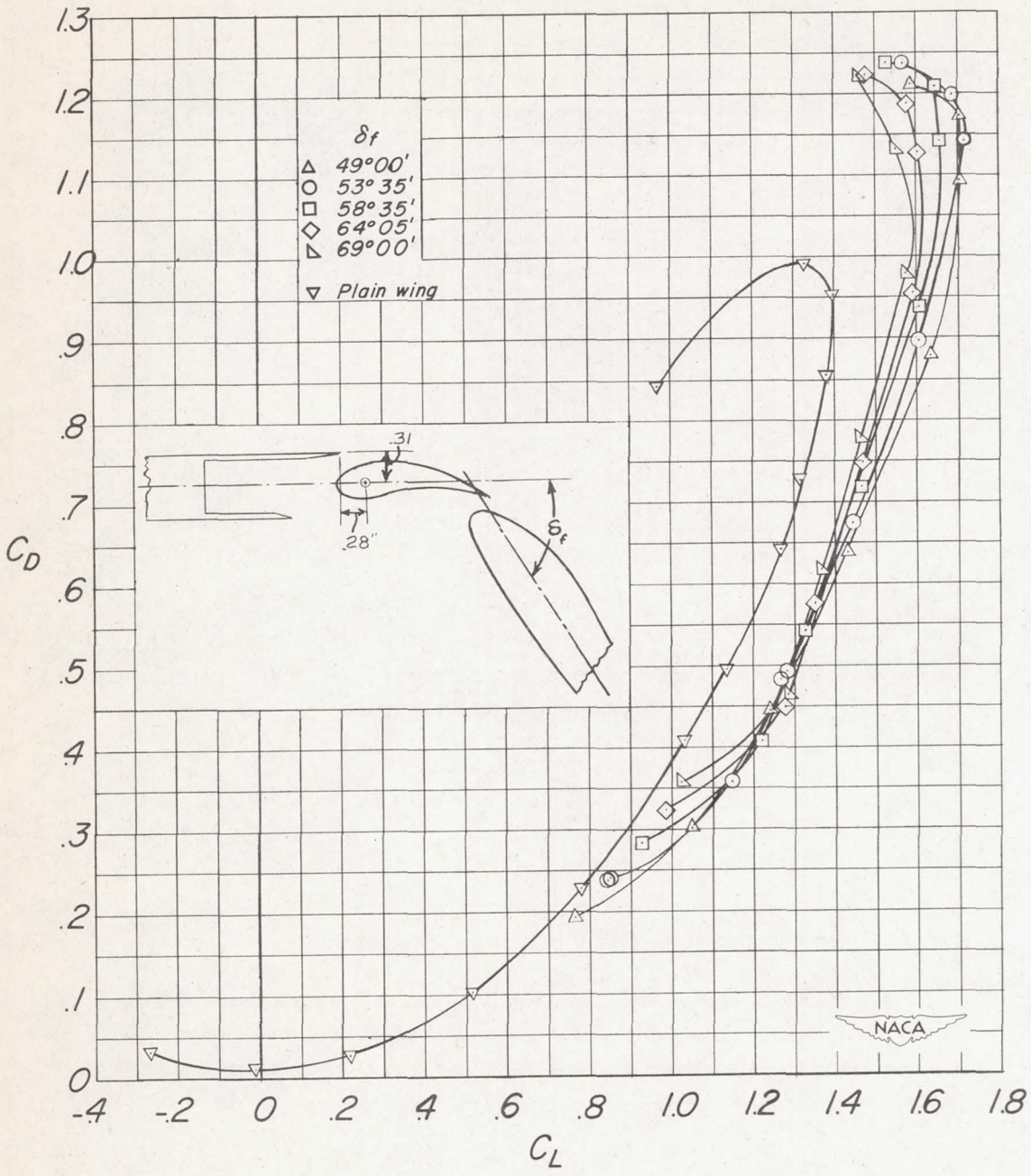

(a) Concluded.

Figure 8.- Continued.

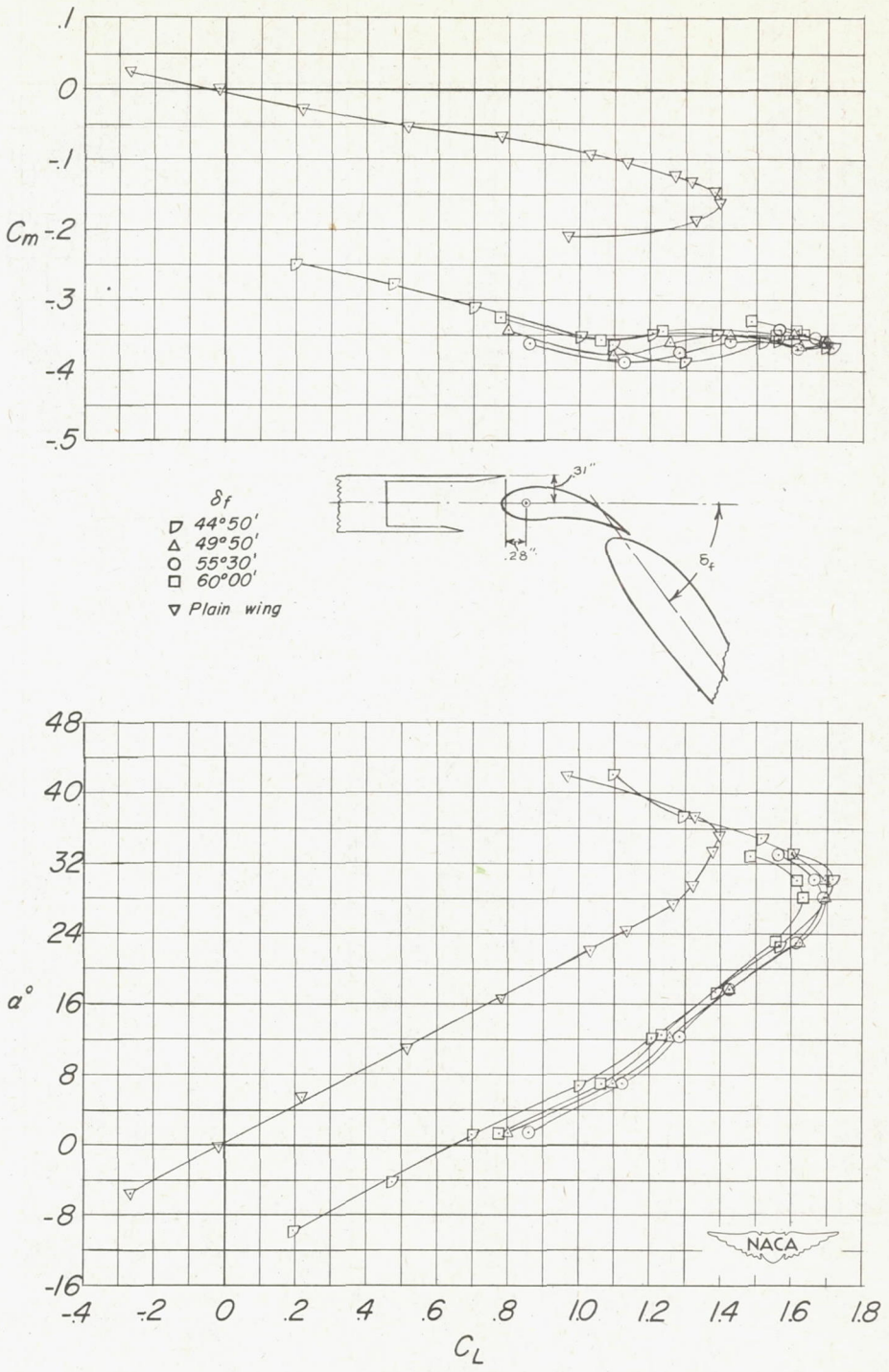

(b) Vane-flap unit B.

Figure 8.- Continued.

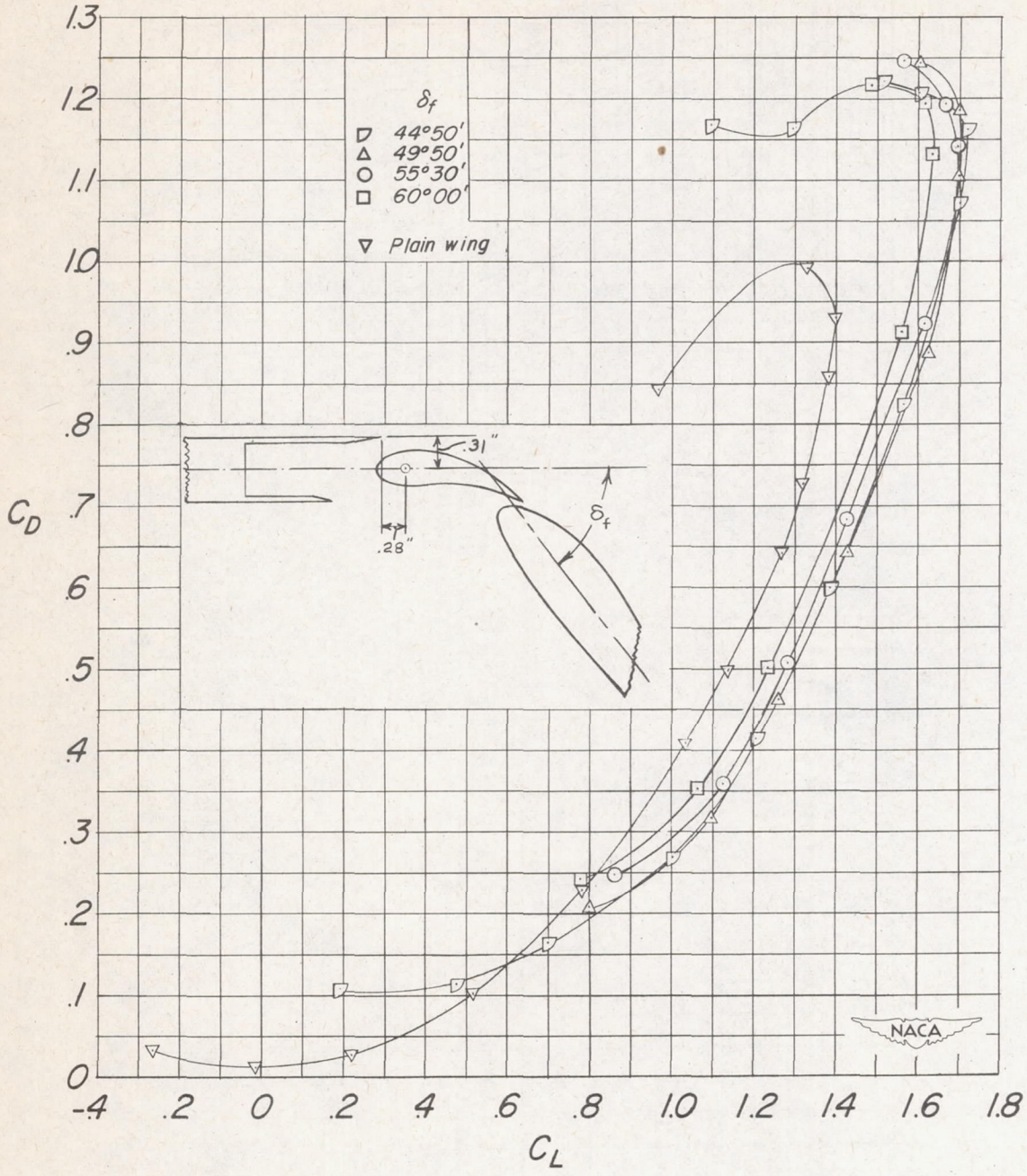

(b) Concluded.

Figure 8.- Continued.

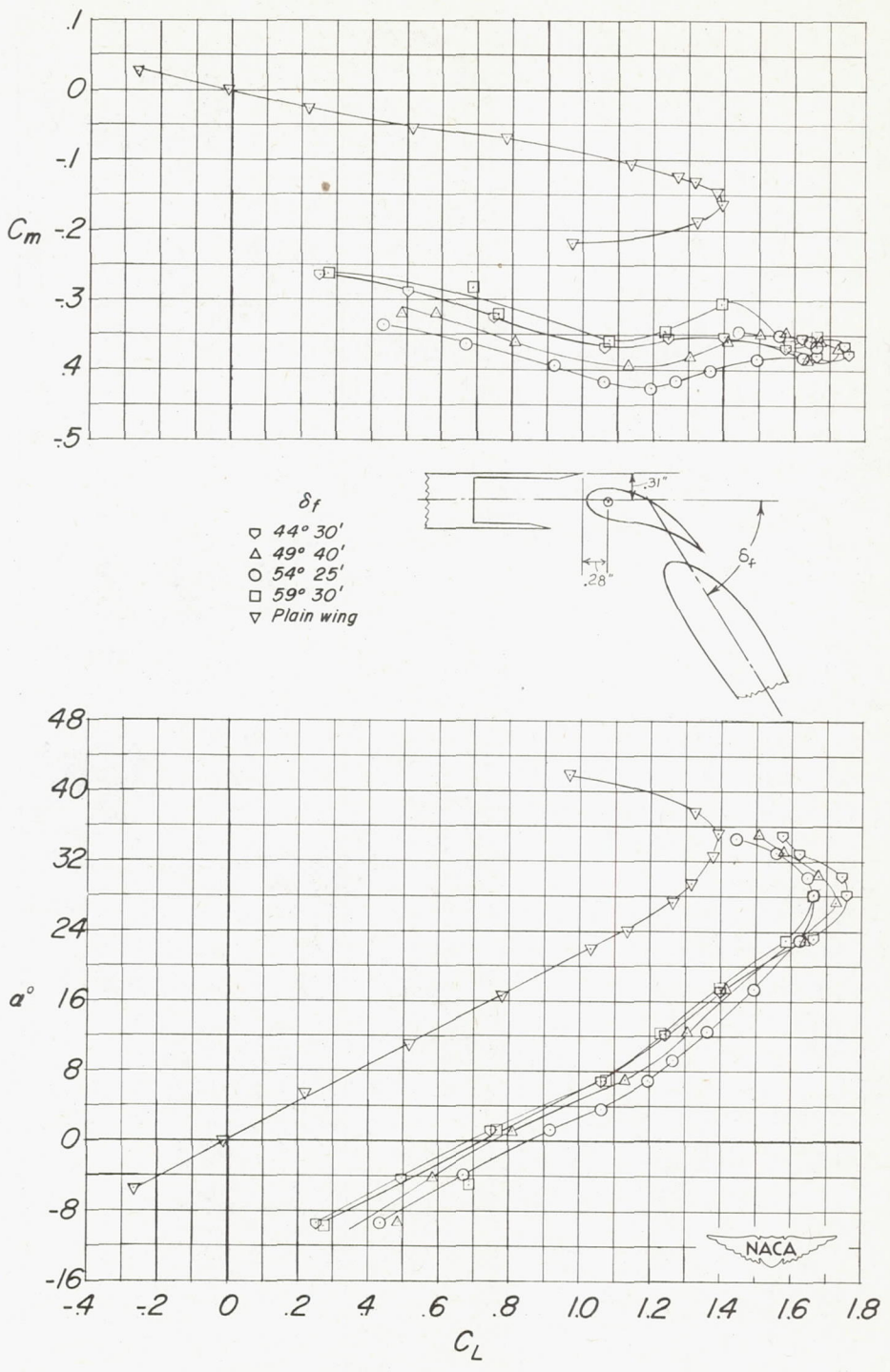

(c) Vane-flap unit C.

Figure 8.- Continued.

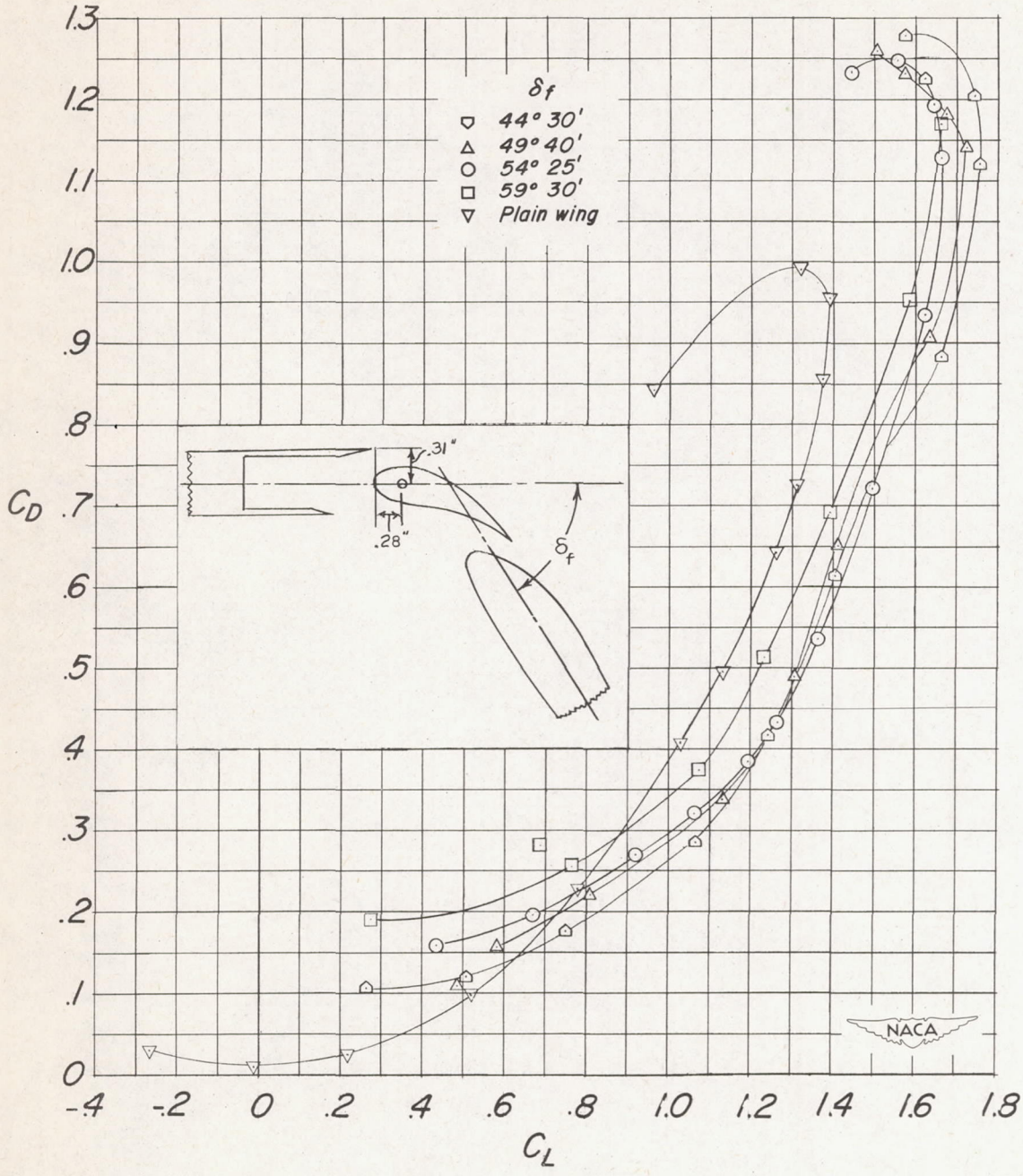

(c) Concluded.

Figure 8.- Continued.

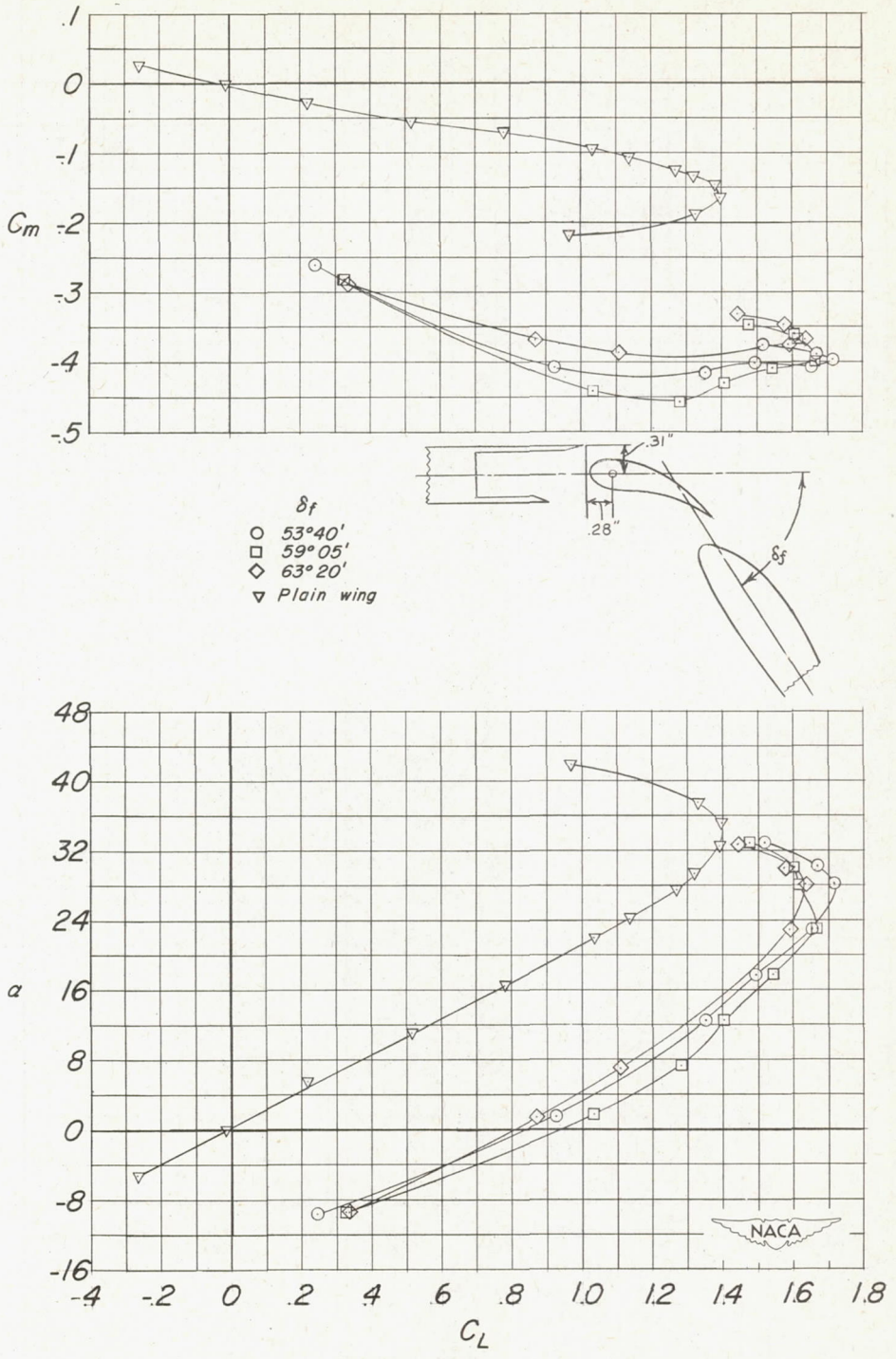

(d) Vane-flap unit D.

Figure 8.- Continued.

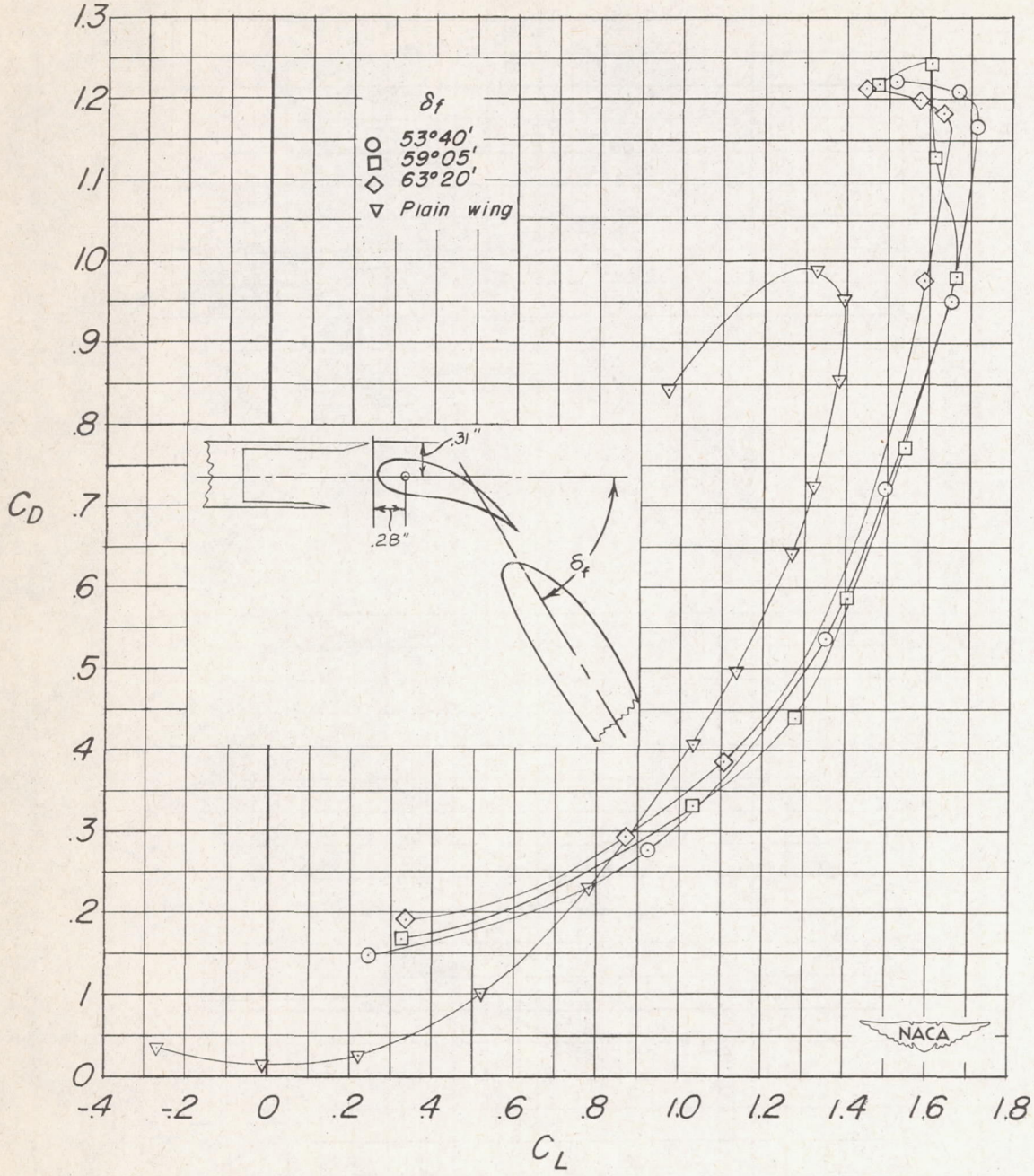

(d) Concluded.

Figure 8.- Continued.

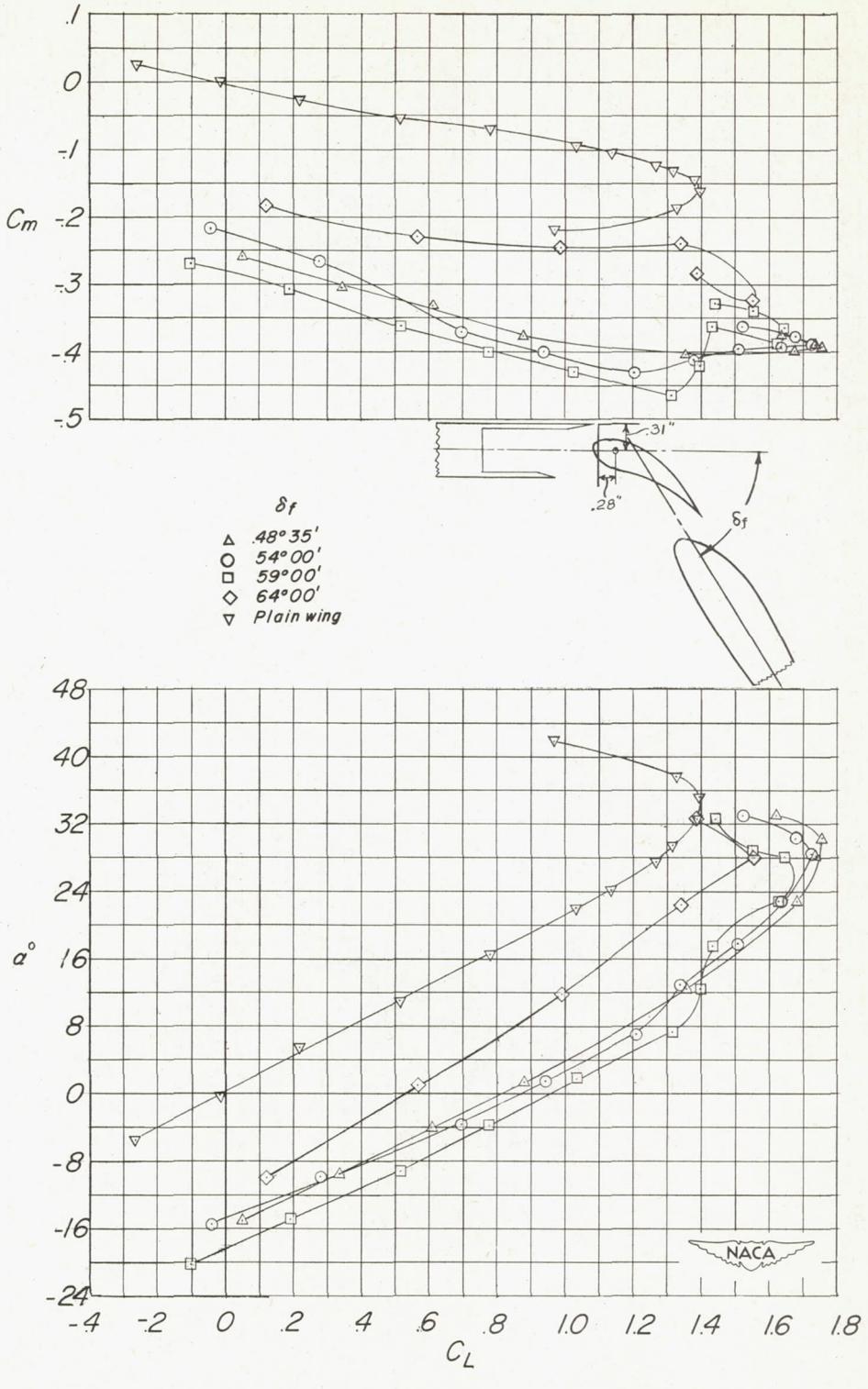

(e) Vane-flap unit E.

Figure 8.- Continued.

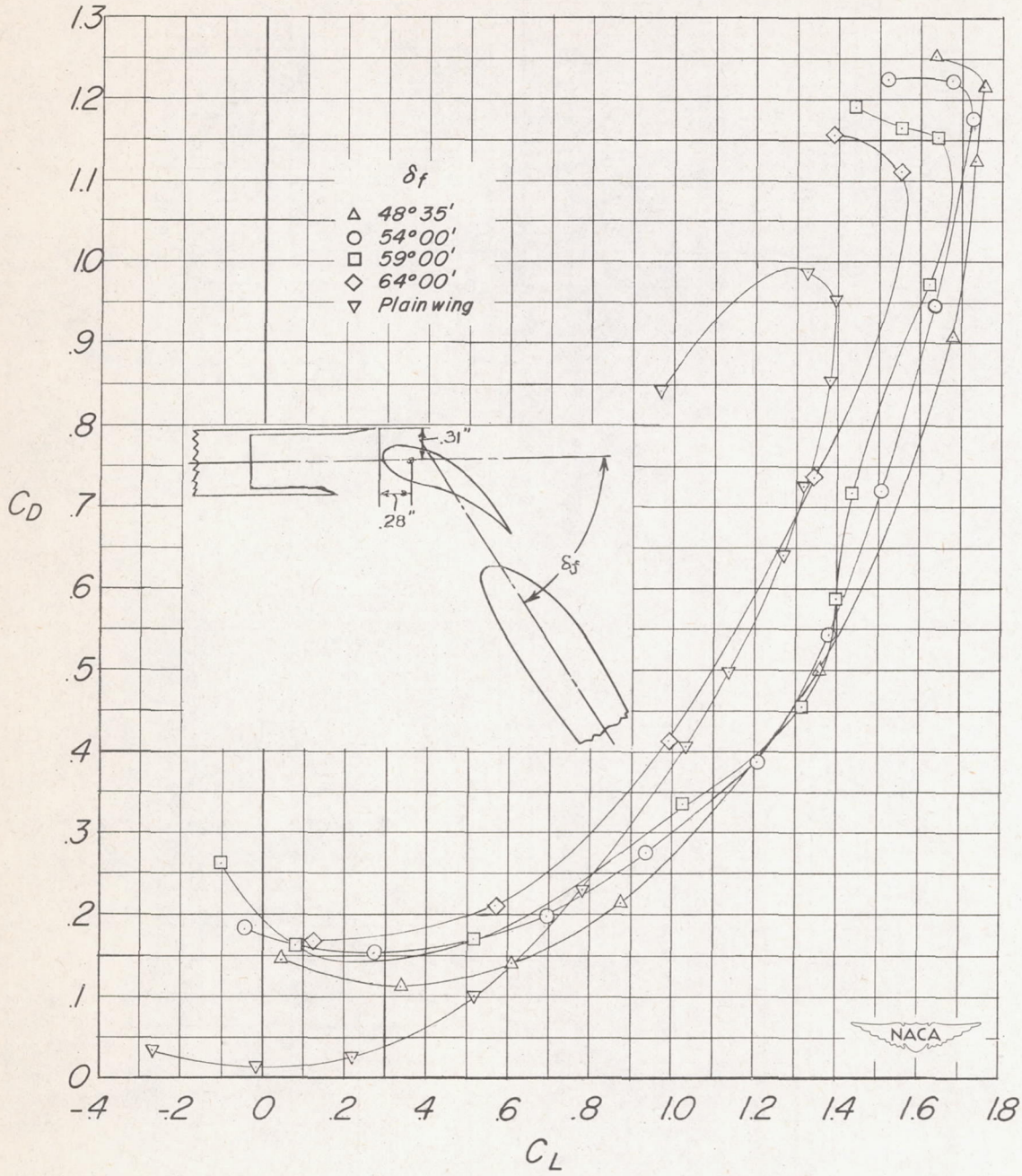

(e) Concluded.

Figure 8.- Concluded.

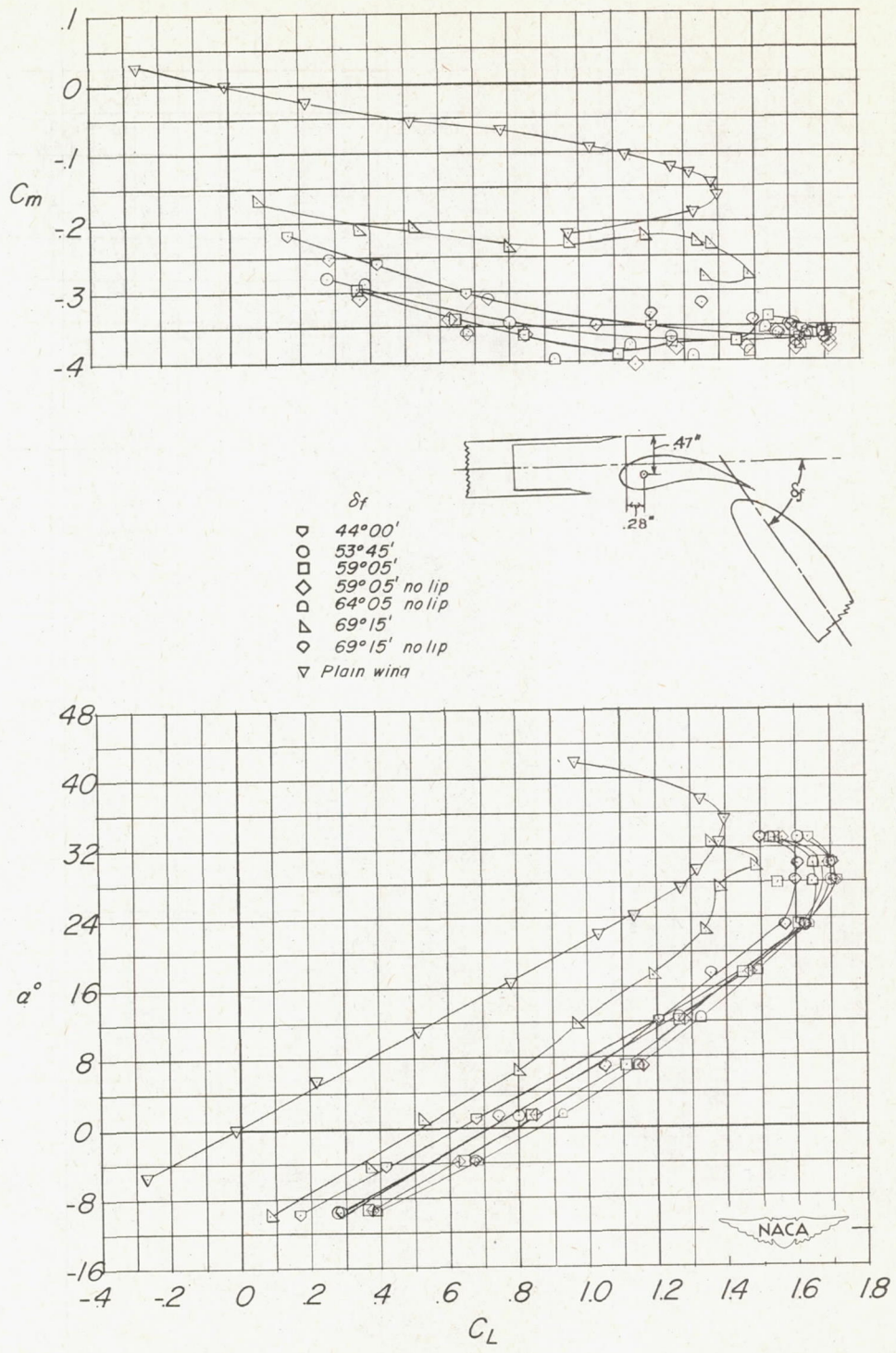

(a) Vane-flap unit A.

Figure 9.- The aerodynamic characteristics of the test model with the vane-flap unit pivoted about point Y.

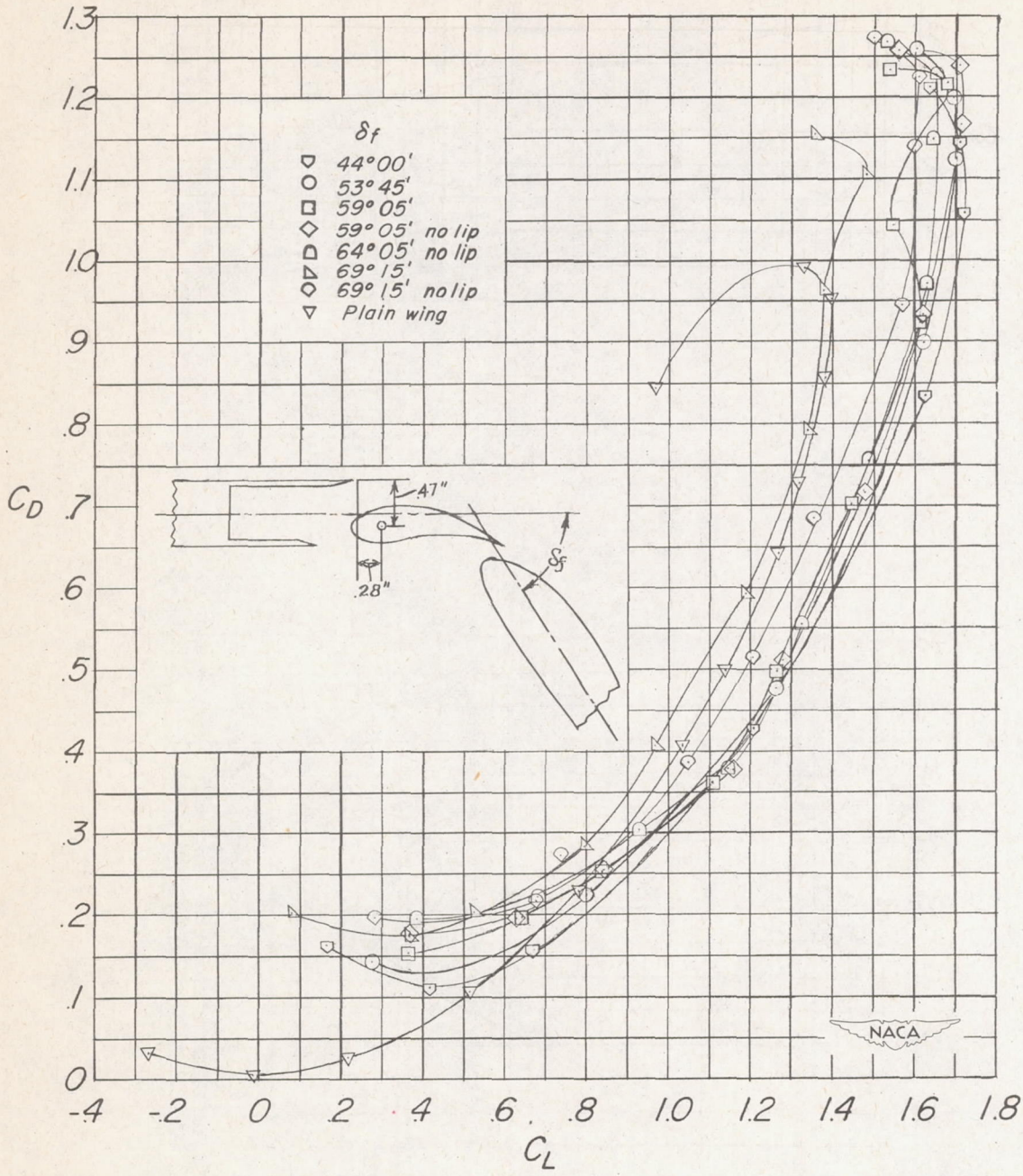

(a) Concluded.

Figure 9.- Continued.

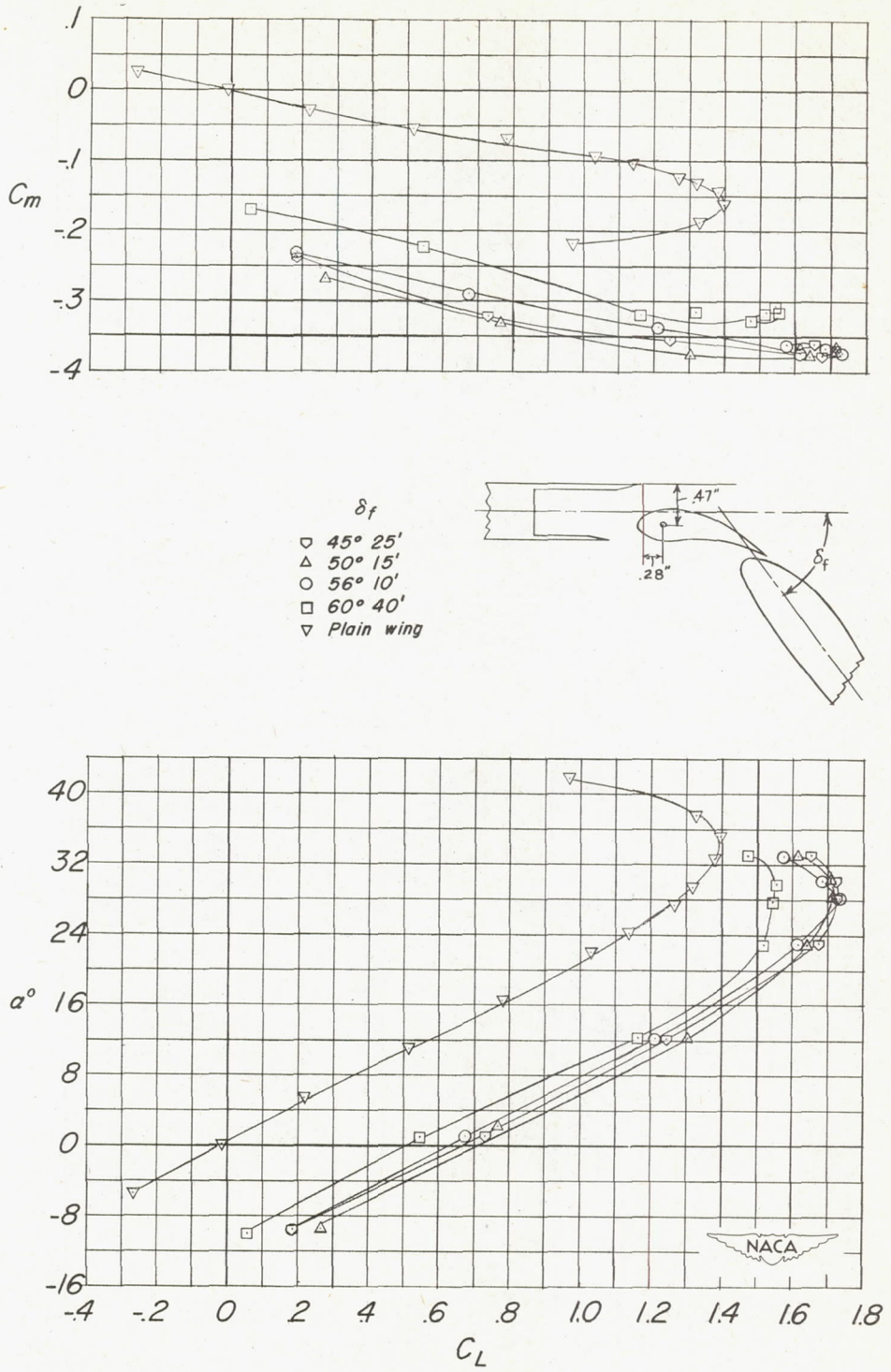

(b) Vane-flap unit B.

Figure 9.- Continued.

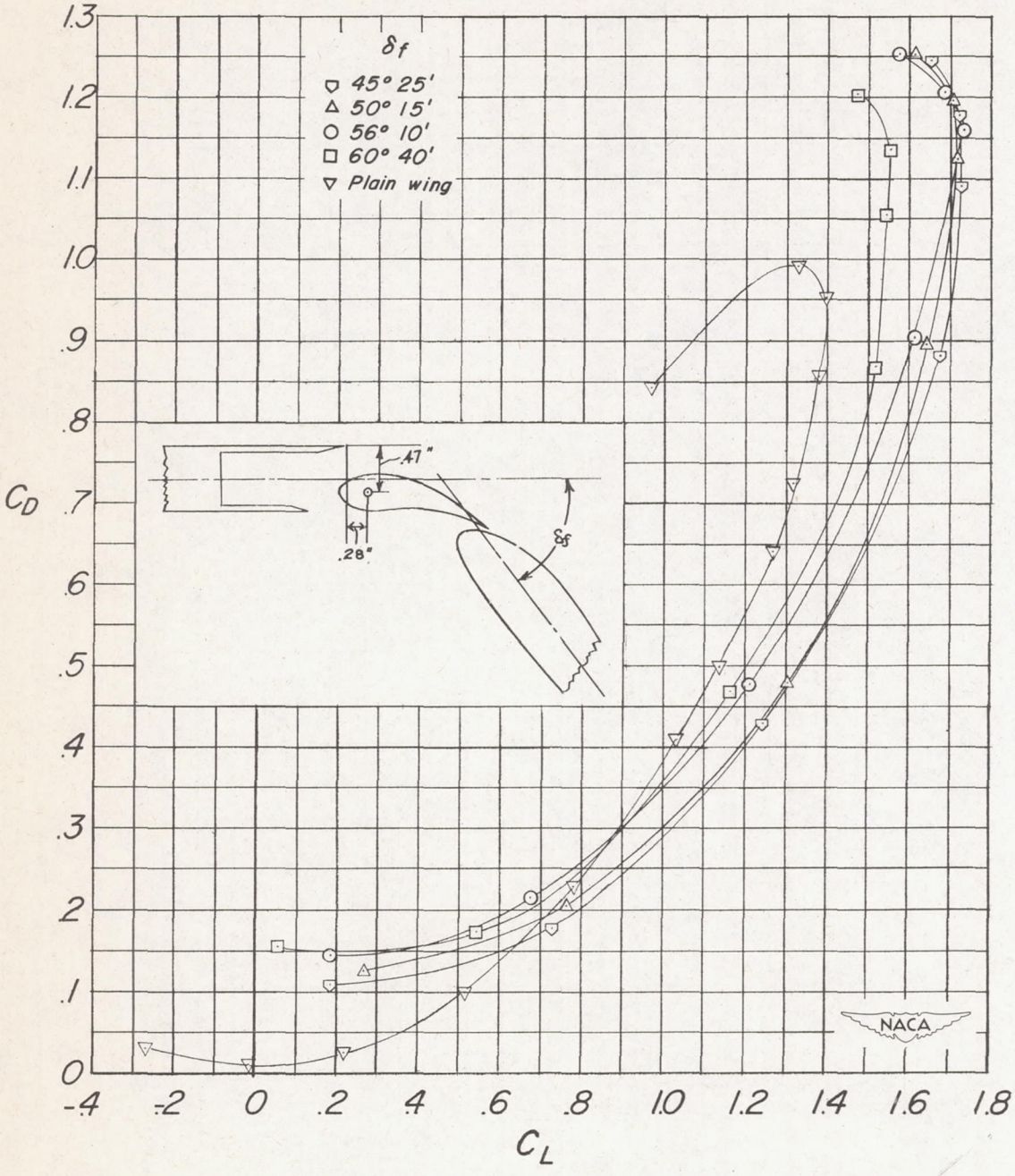

(b) Concluded.

Figure 9.- Continued.

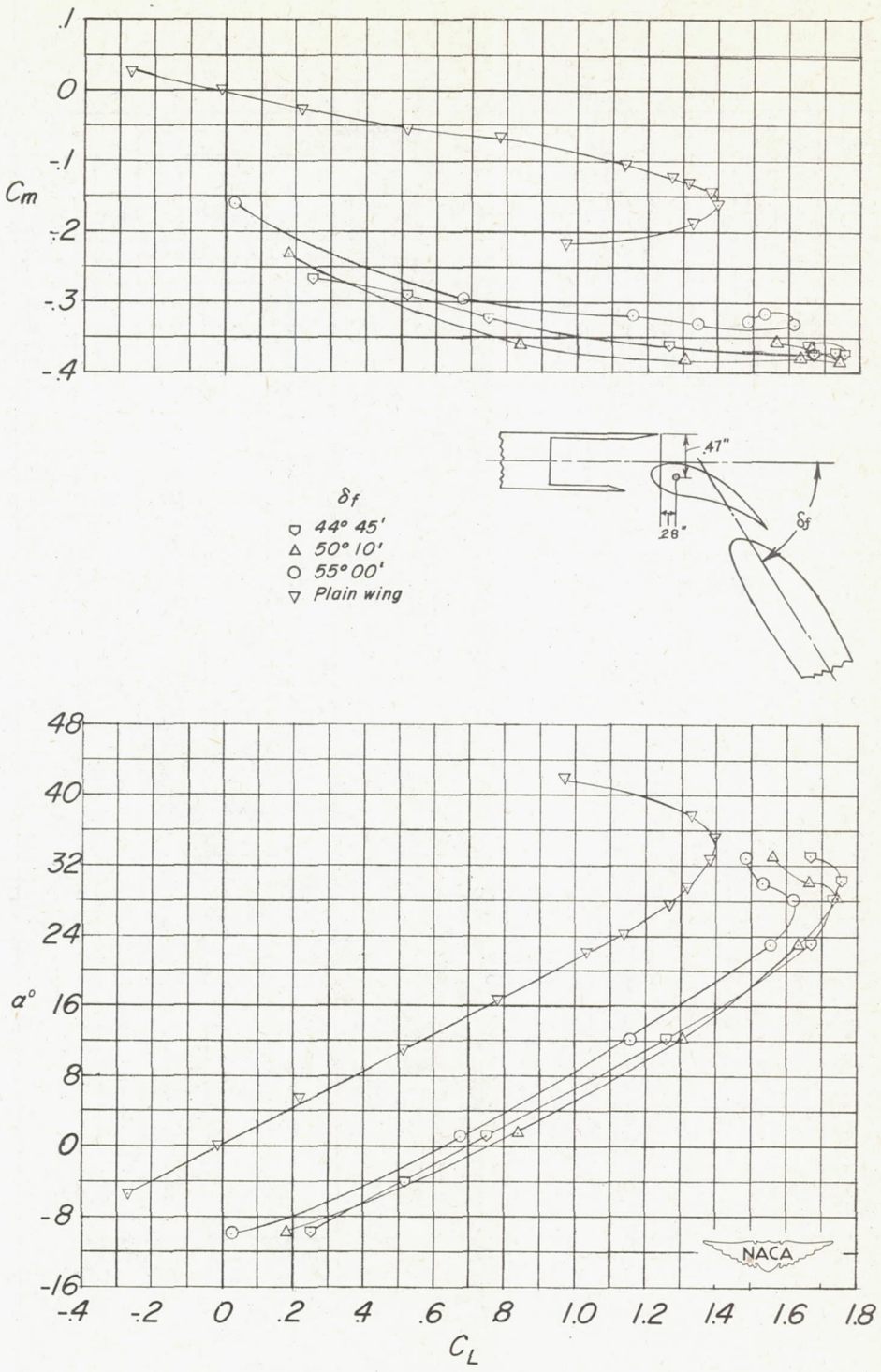

(c) Vane-flap unit C.

Figure 9.- Continued.

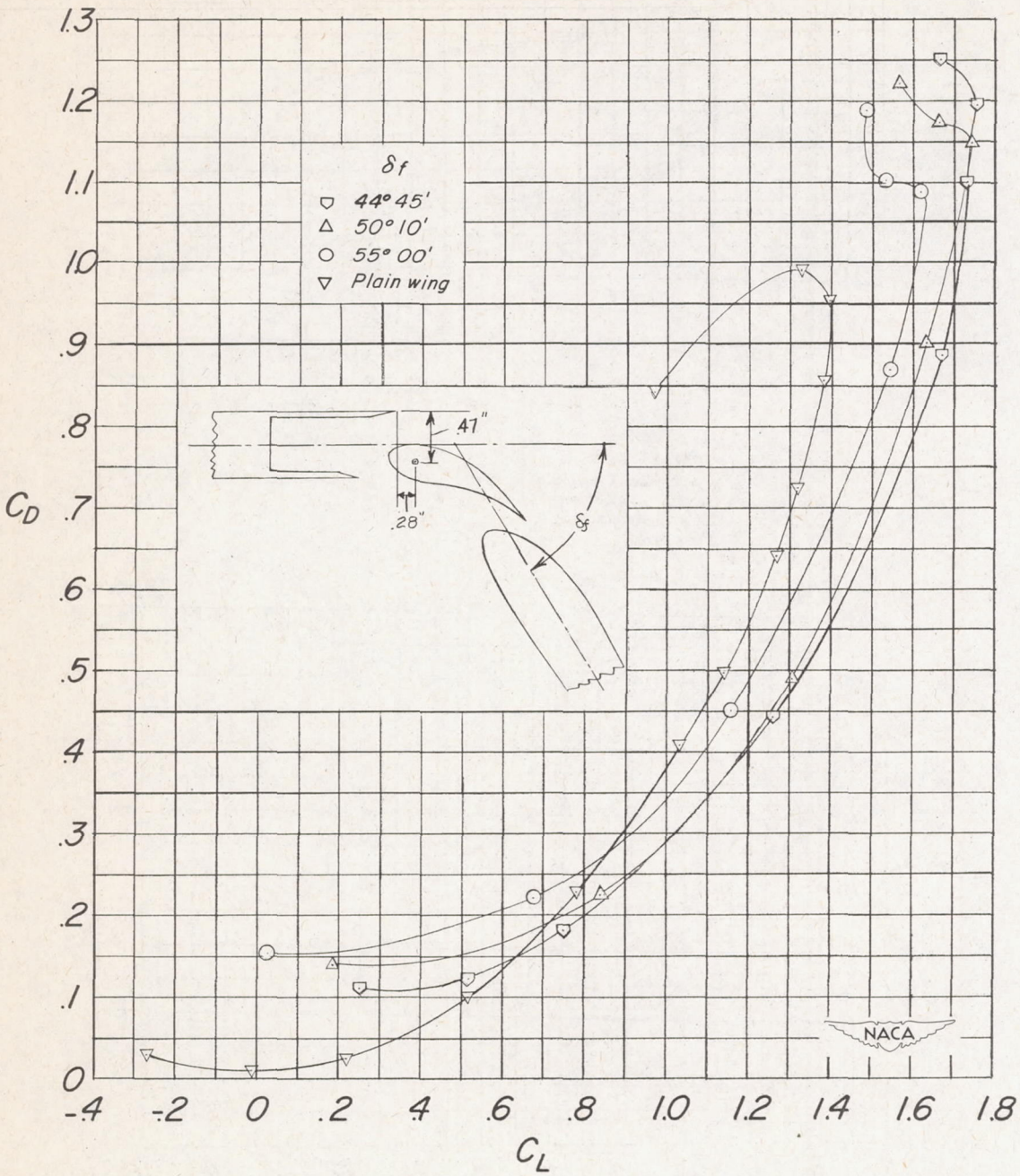

(c) Concluded.

Figure 9.- Continued.

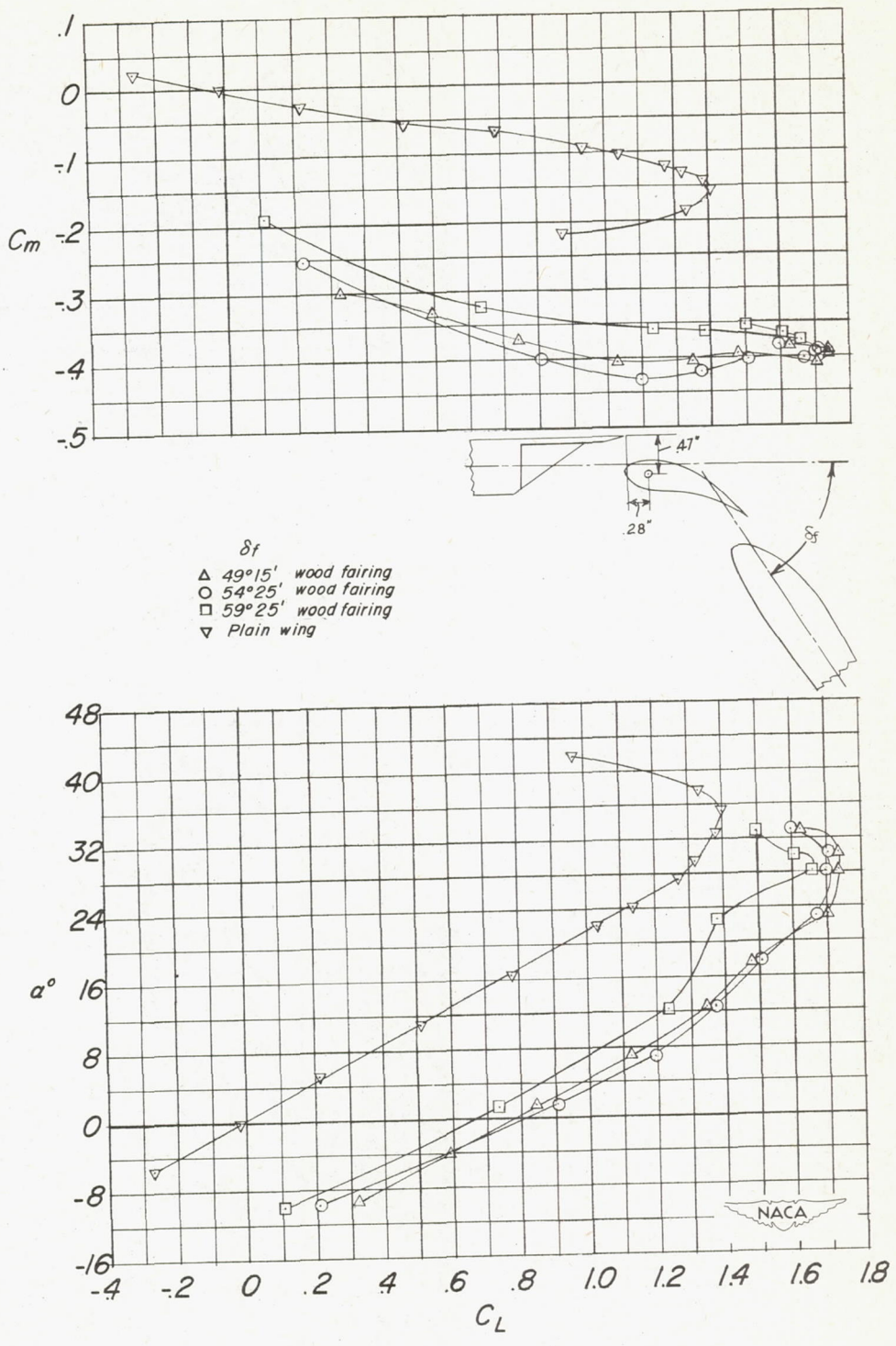

(d) Vane-flap unit D.

Figure 9.- Continued.

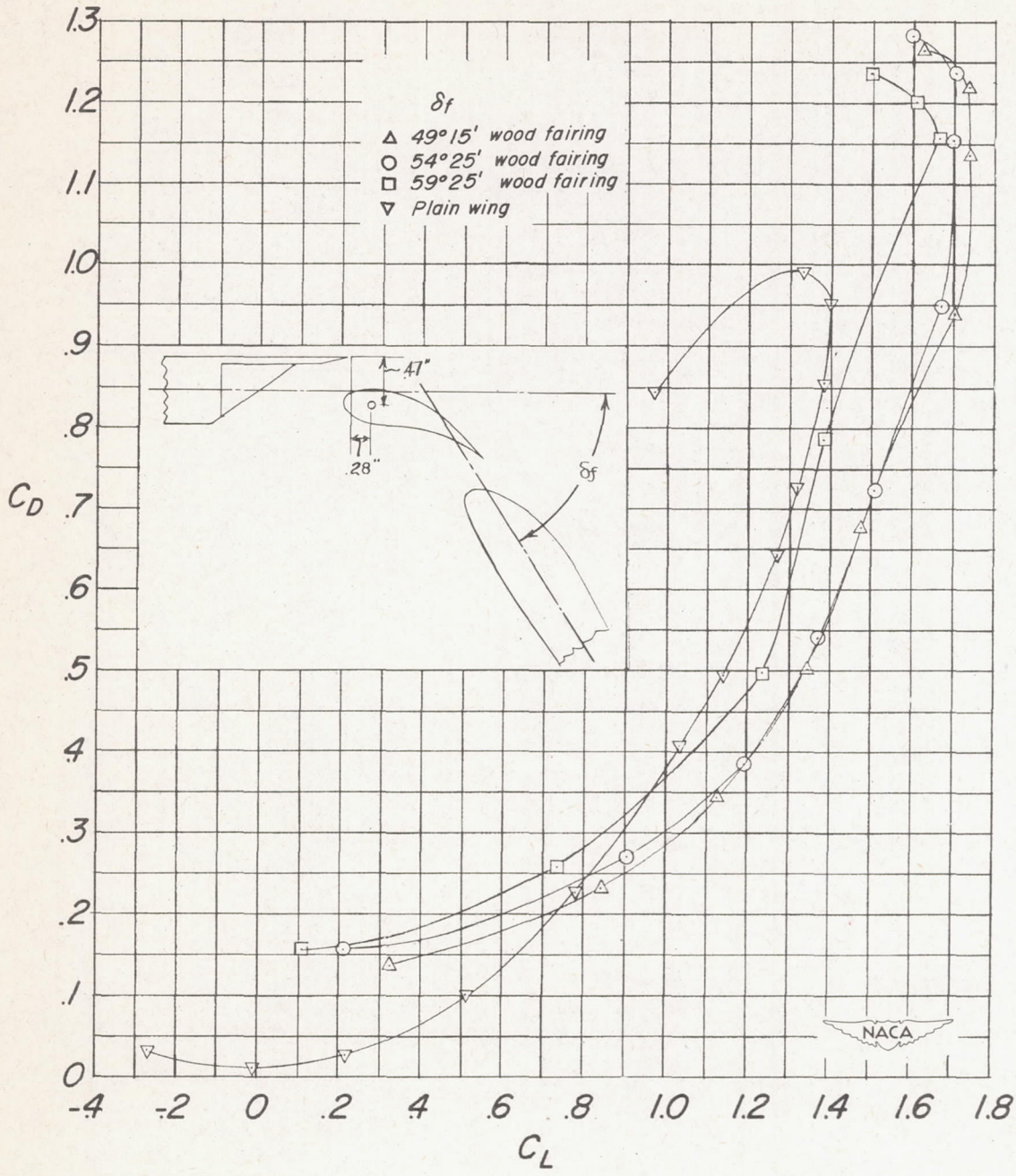

(d) Concluded.

Figure 9.- Continued.

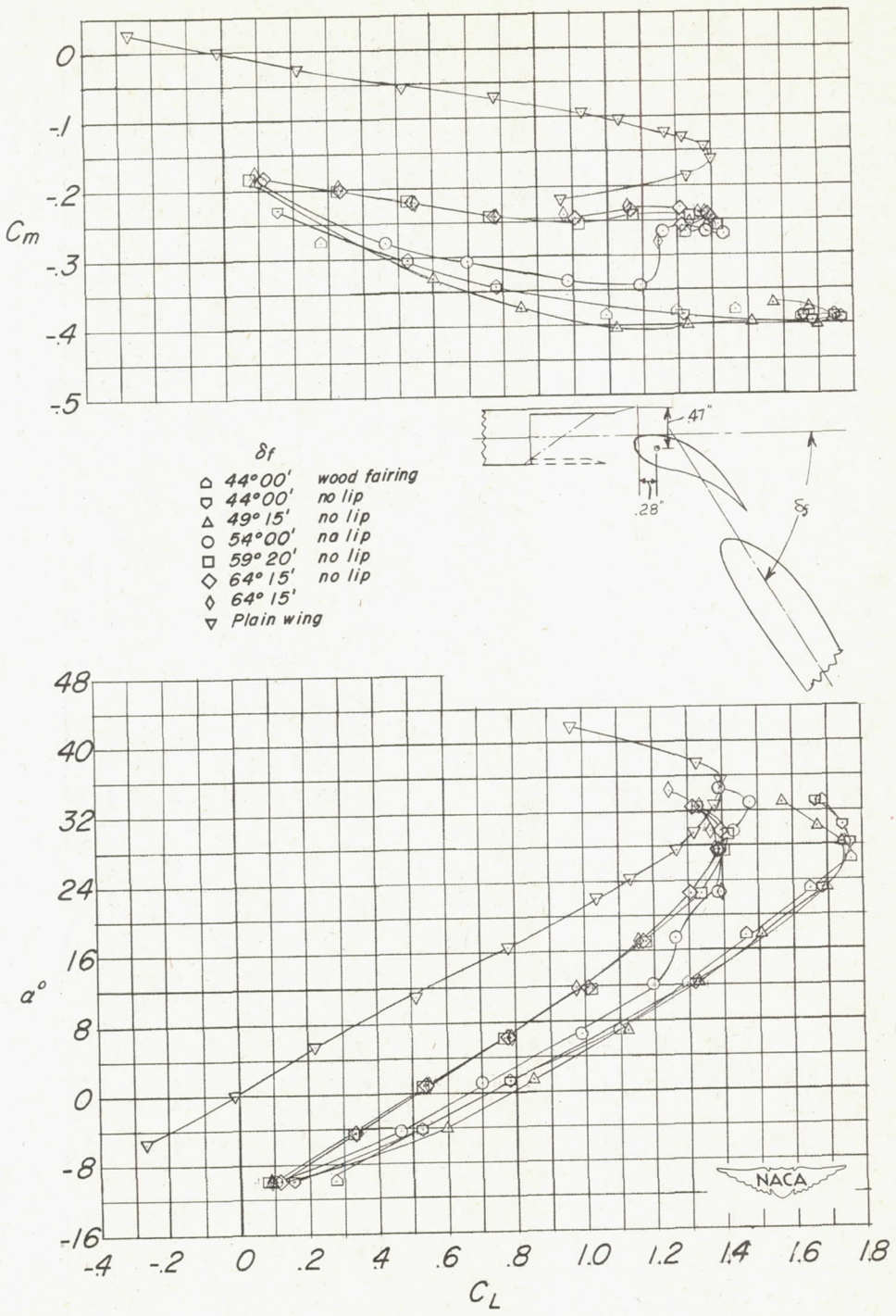

(e) Vane-flap unit E.

Figure 9.- Continued.

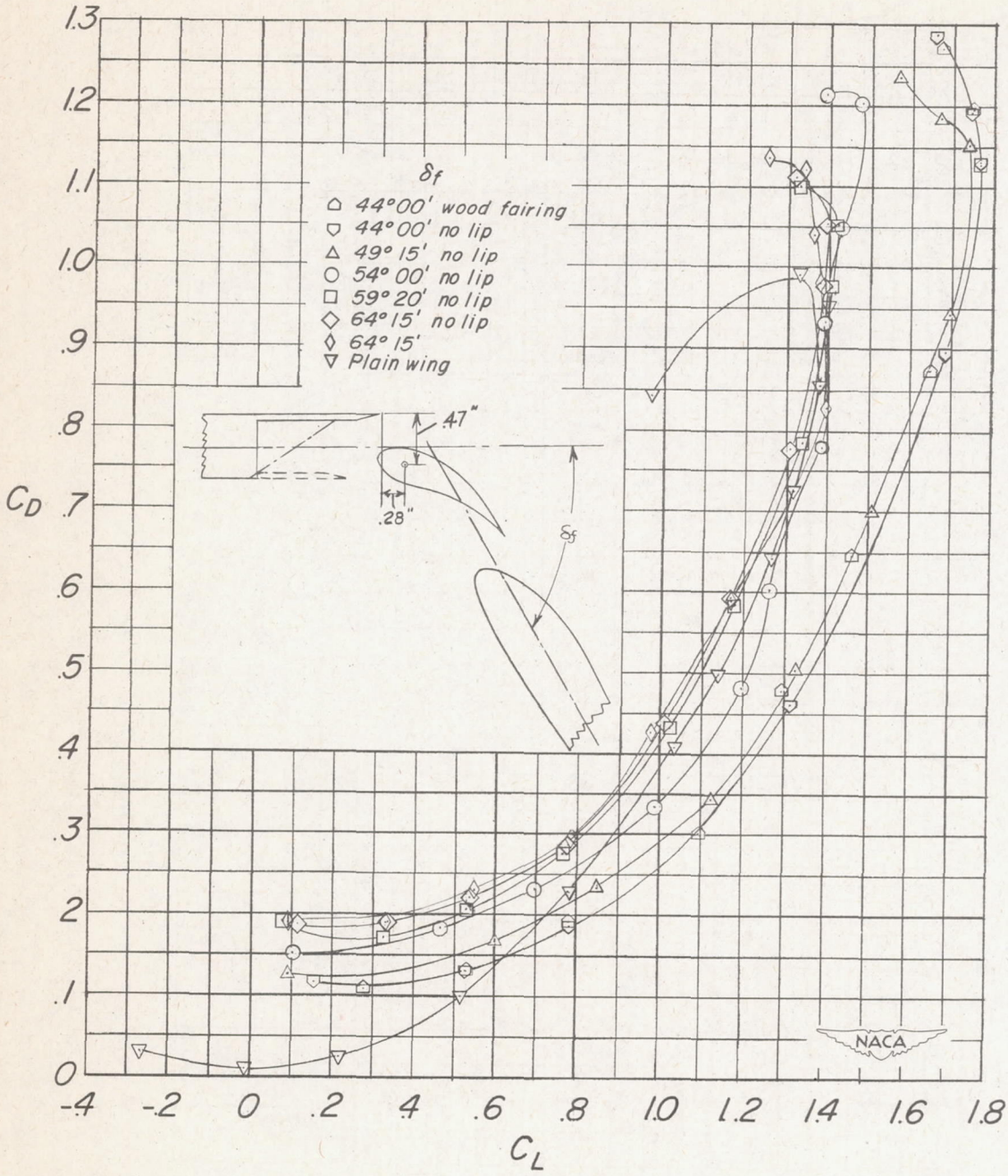

(e) Concluded.

Figure 9.- Concluded.

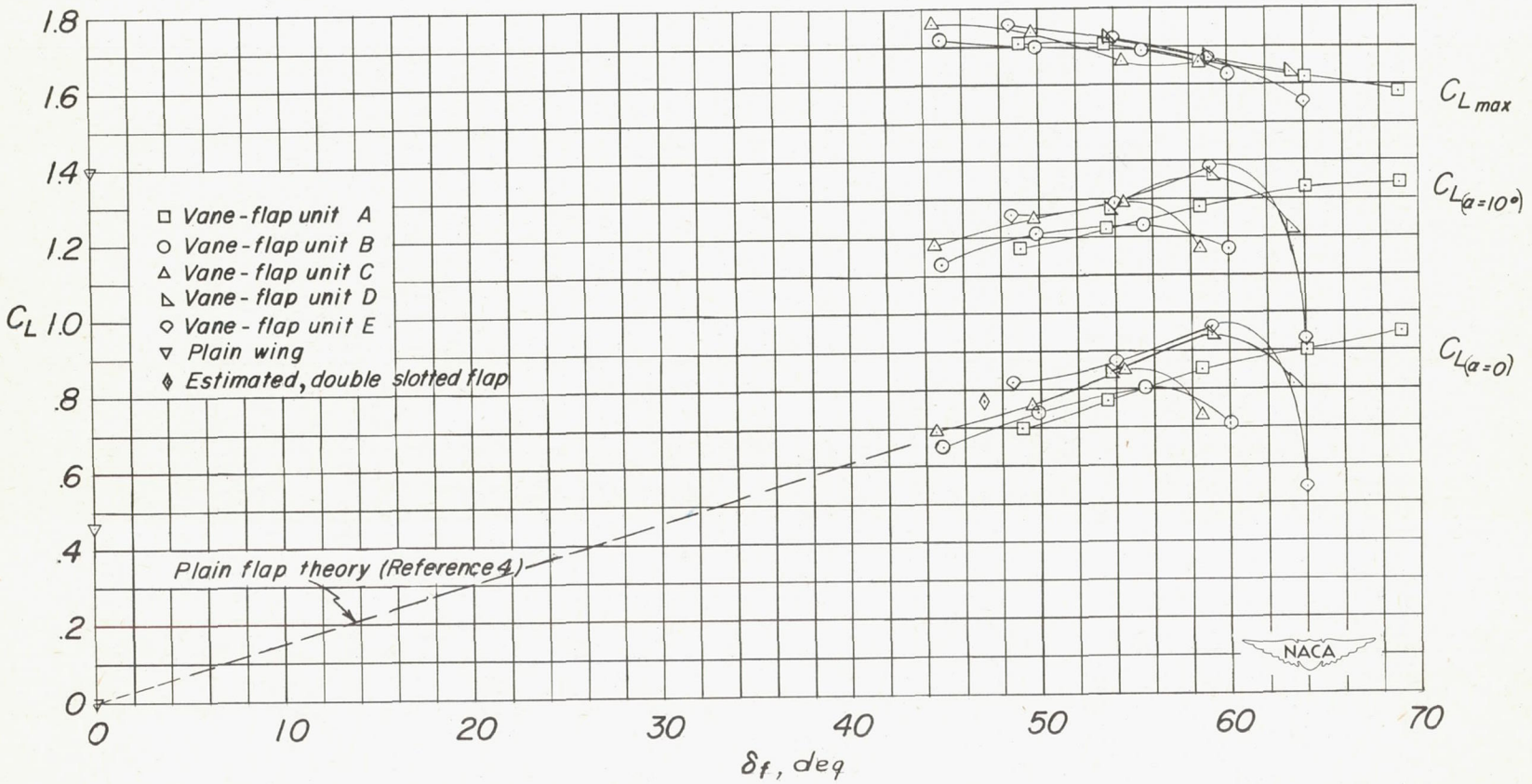

(a) Pivot point X.

Figure 10.- The variation of C_L at $\alpha = 0^\circ$, C_L at $\alpha = 10^\circ$, and $C_{L_{max}}$ with deflection of the double slotted flap.

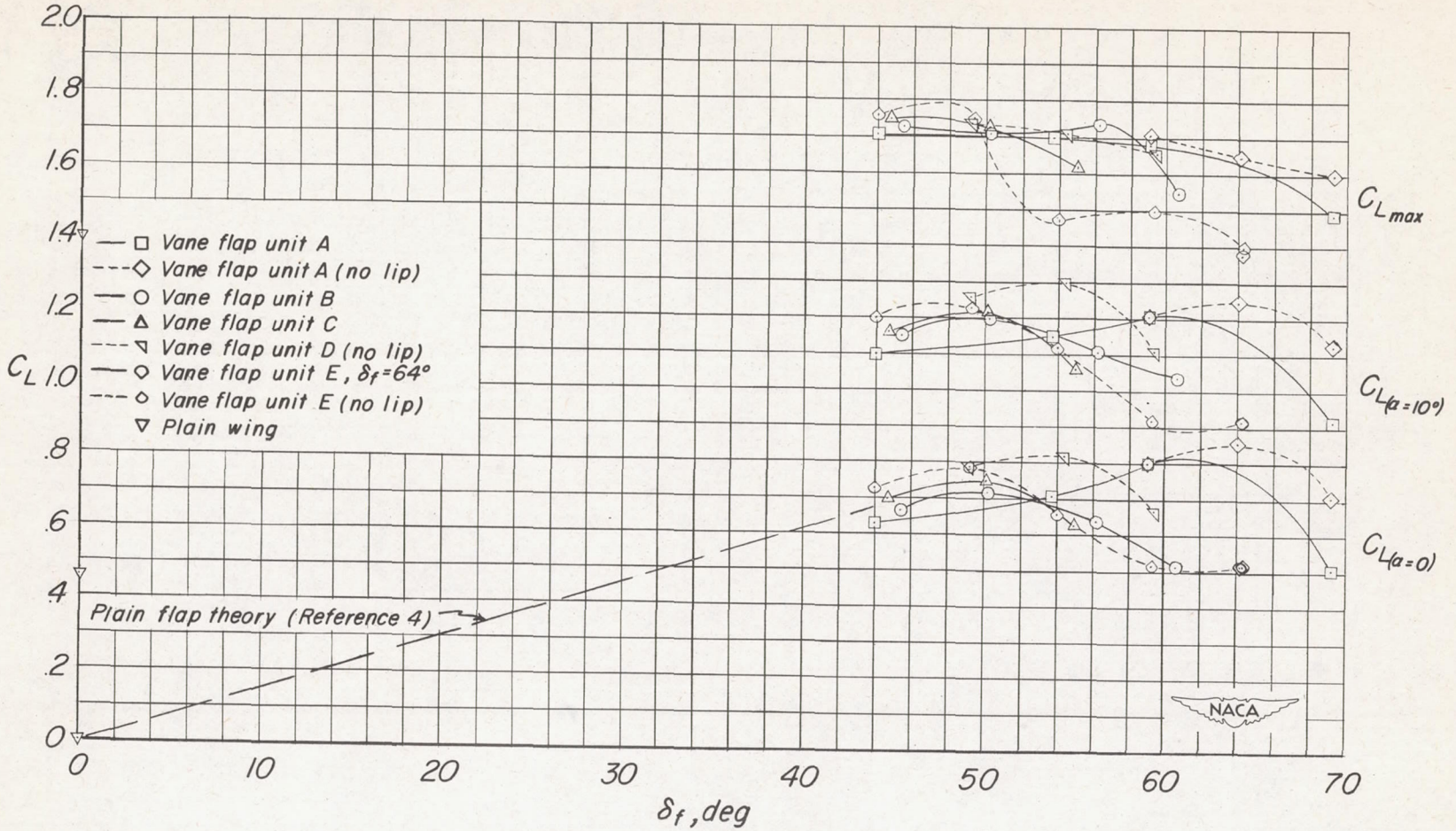

(b) Pivot point Y.

Figure 10.- Concluded.

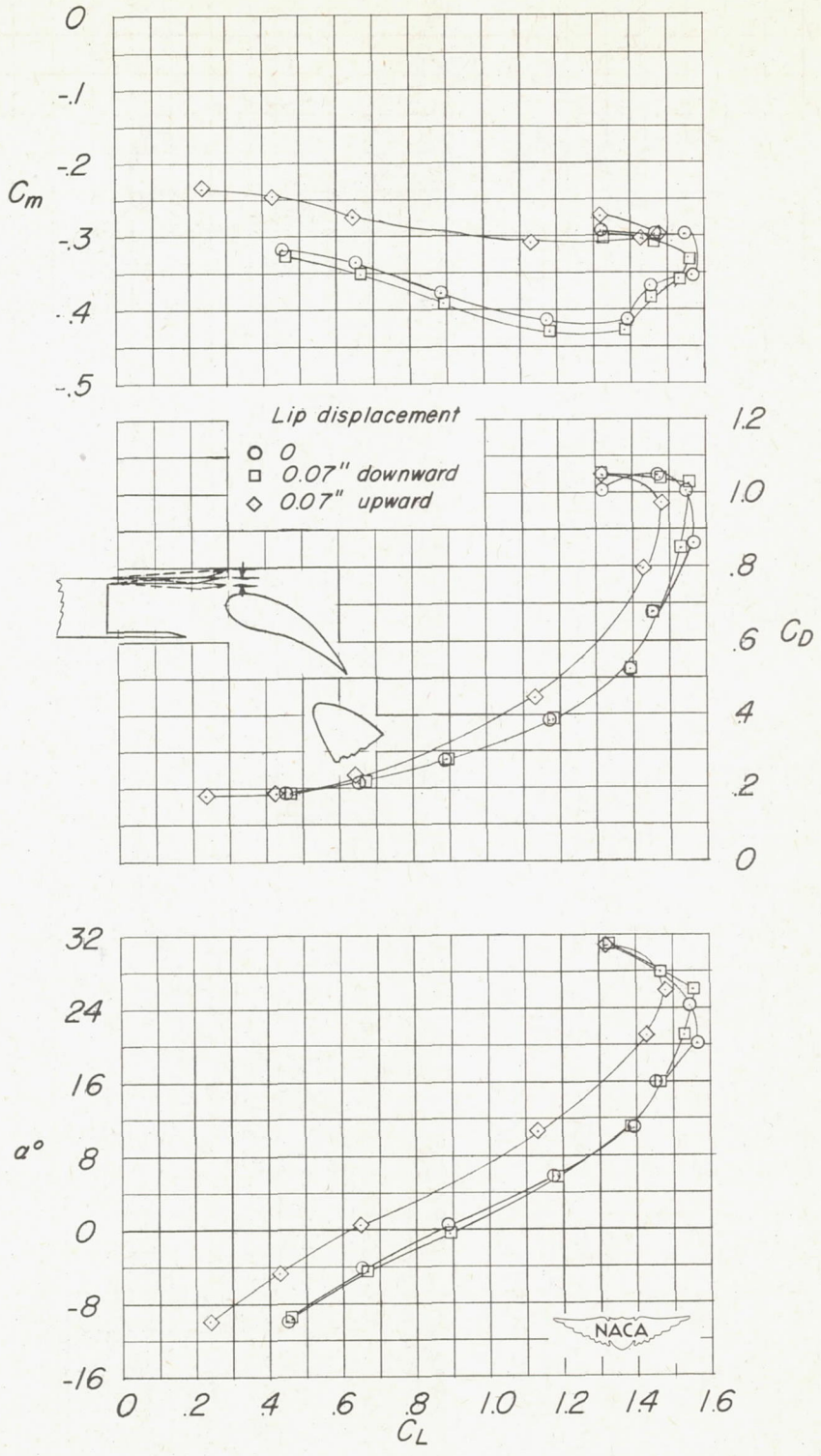

Figure 11.- Effect of deflecting the lip on the model with vane-flap unit E at pivot point X with $\delta_f = 59°00'$.

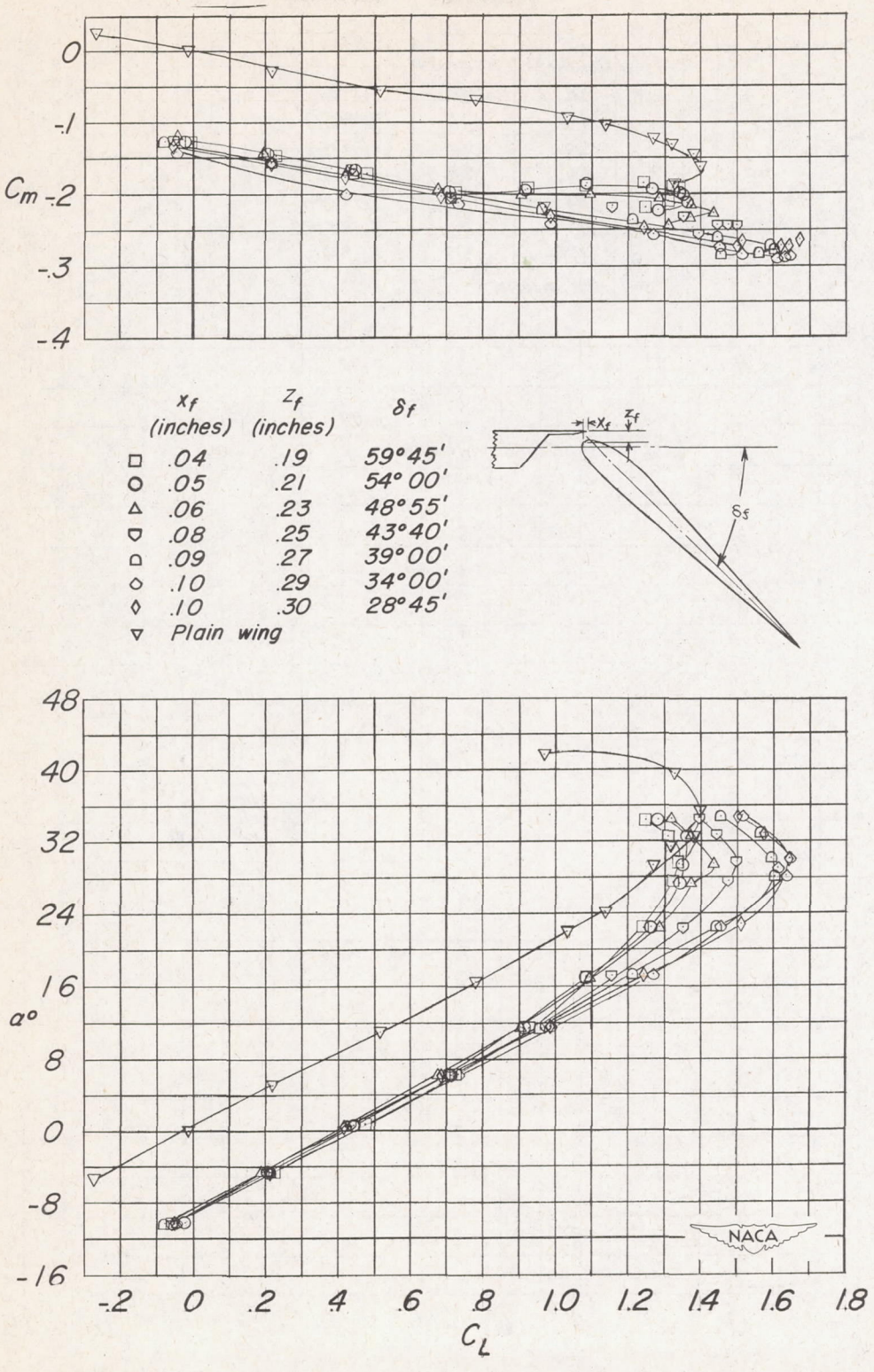

Figure 12.- The aerodynamic characteristics of the test model equipped with a single slotted flap.

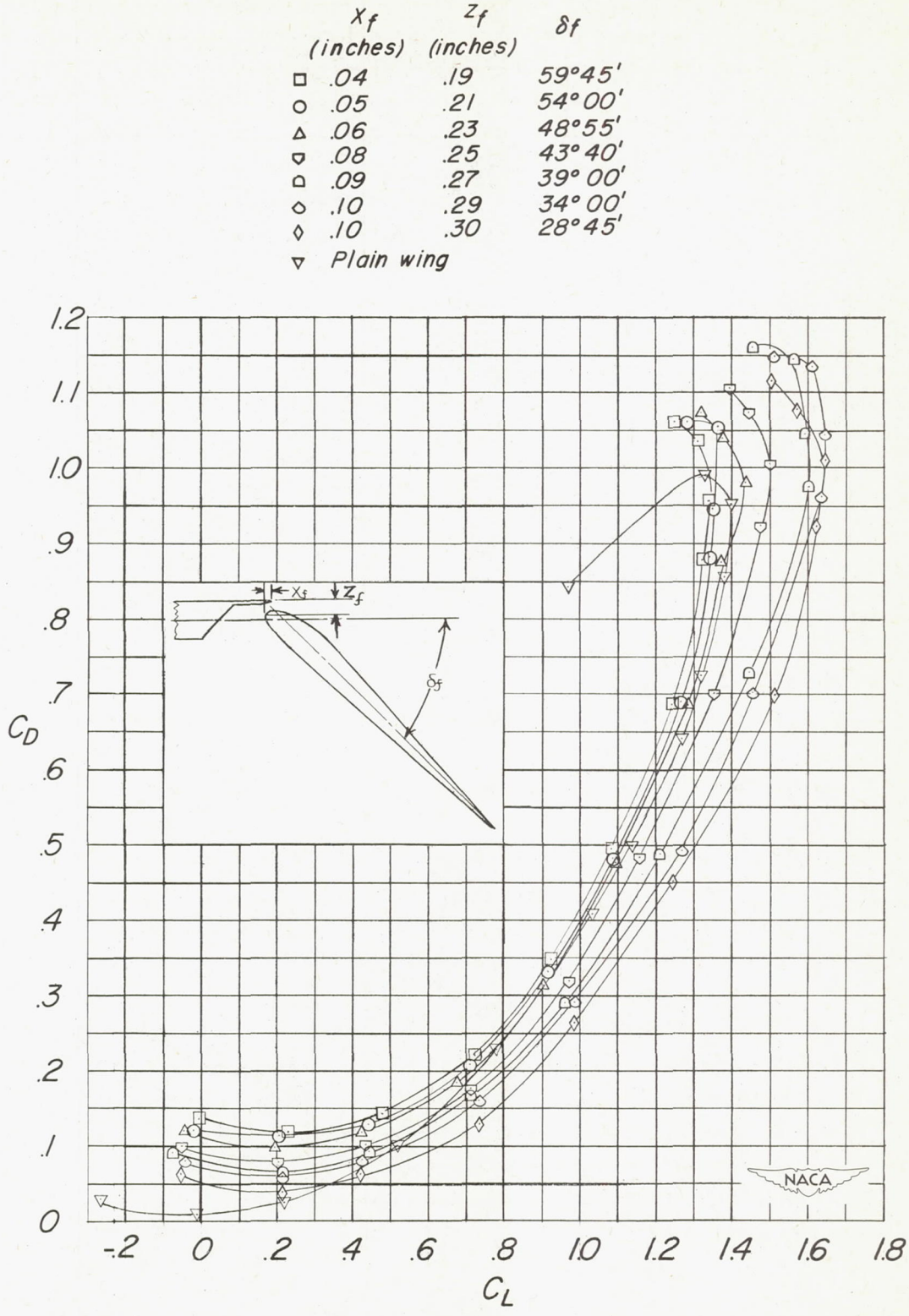

Figure 12.- Concluded.

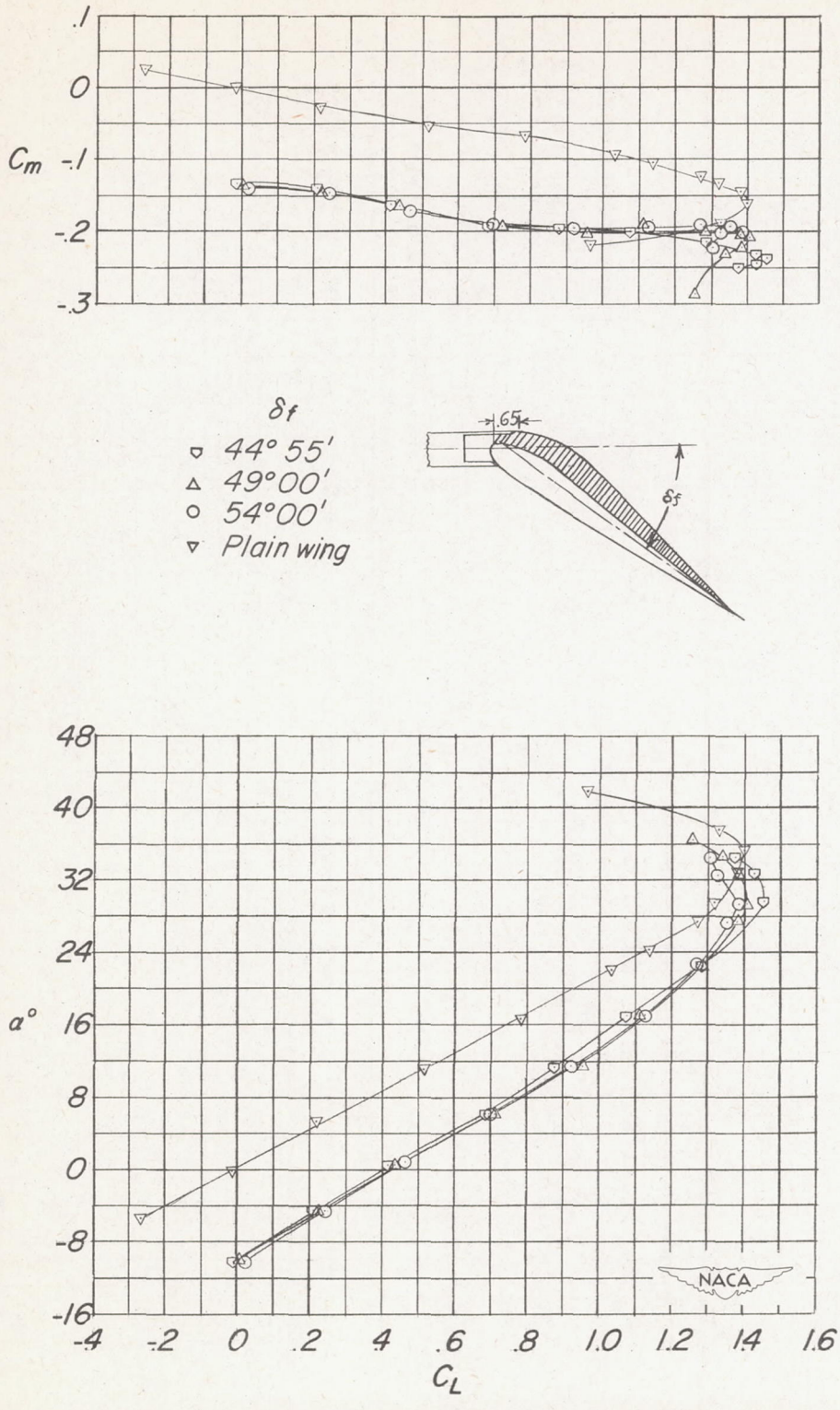

Figure 13.- The aerodynamic characteristics of the test model equipped with a plain flap.

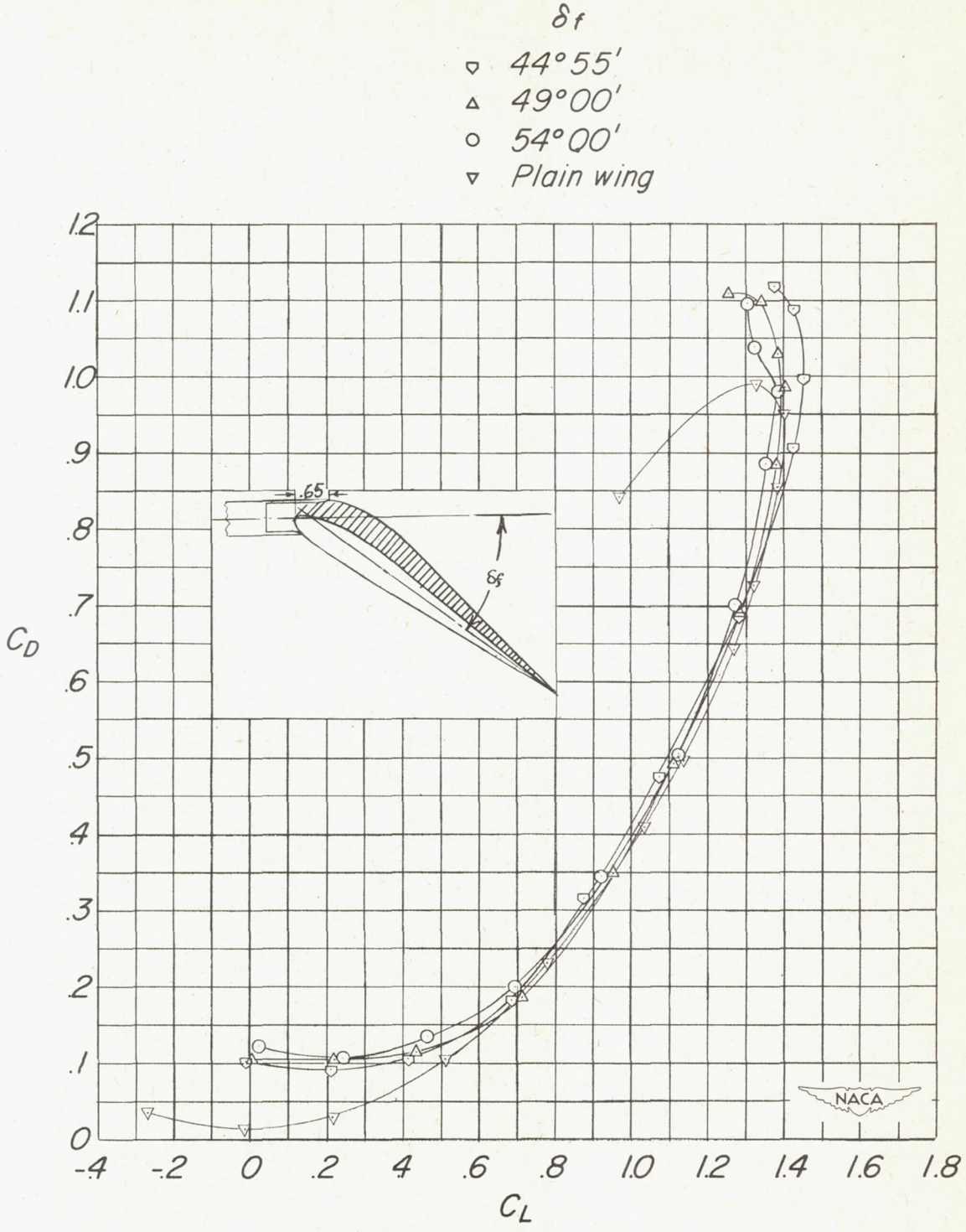

Figure 13.- Concluded.

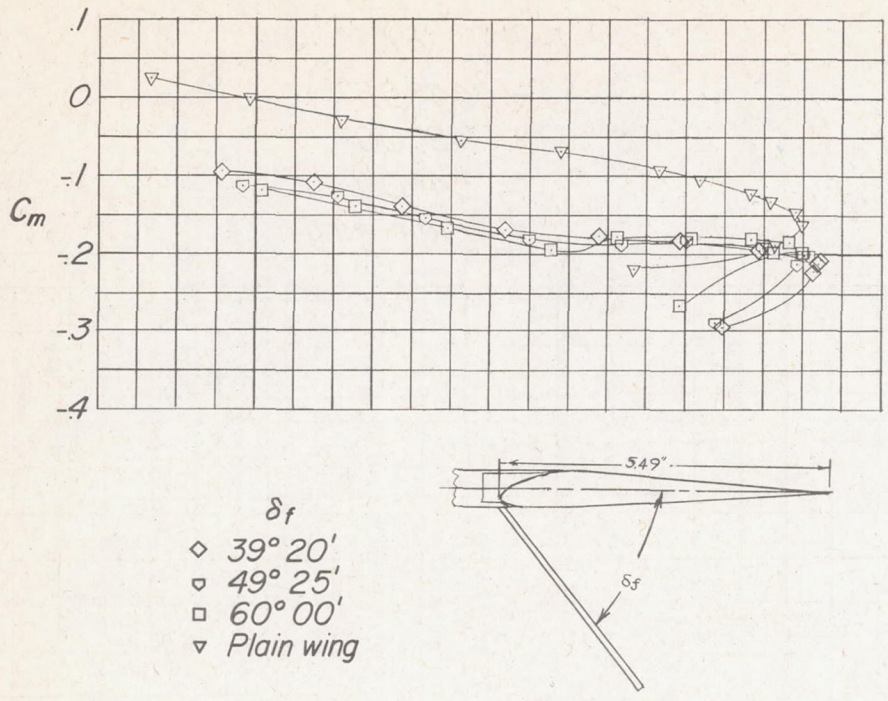

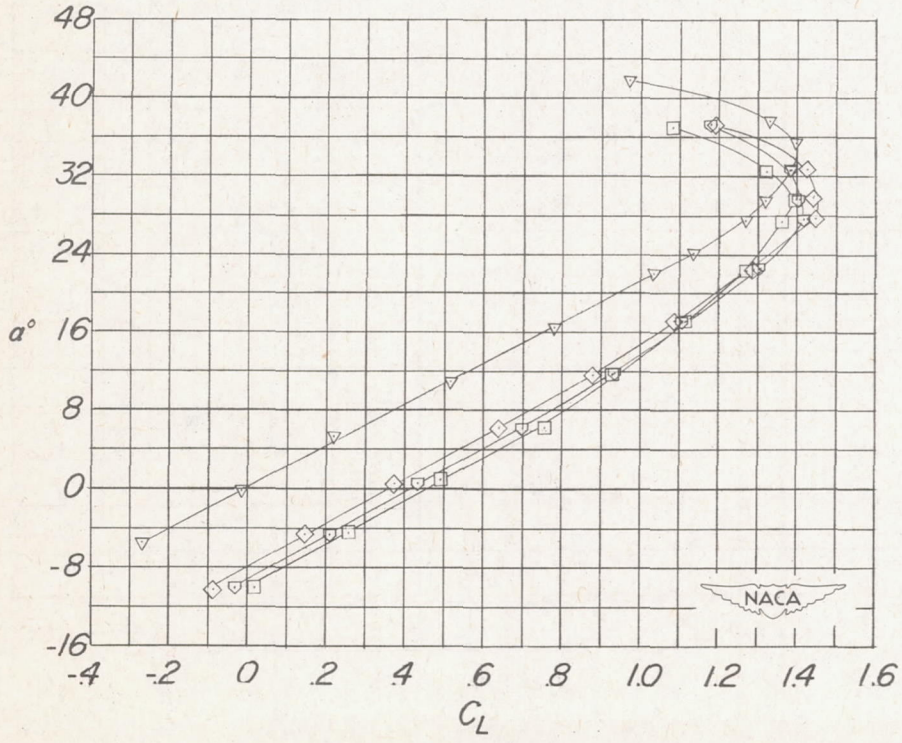

Figure 14.- The aerodynamic characteristics of the test model equipped with a split flap.

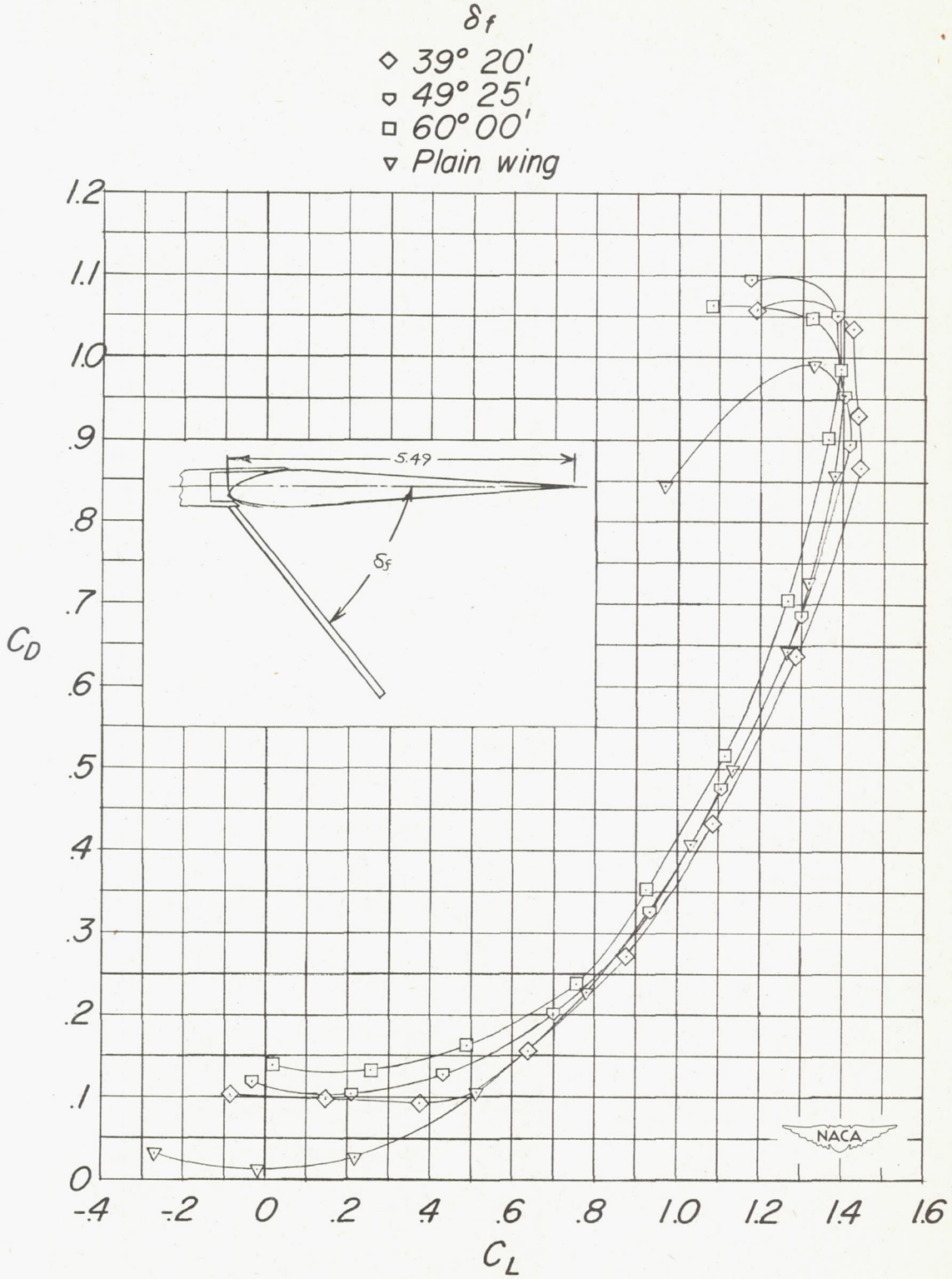

Figure 14.- Concluded.

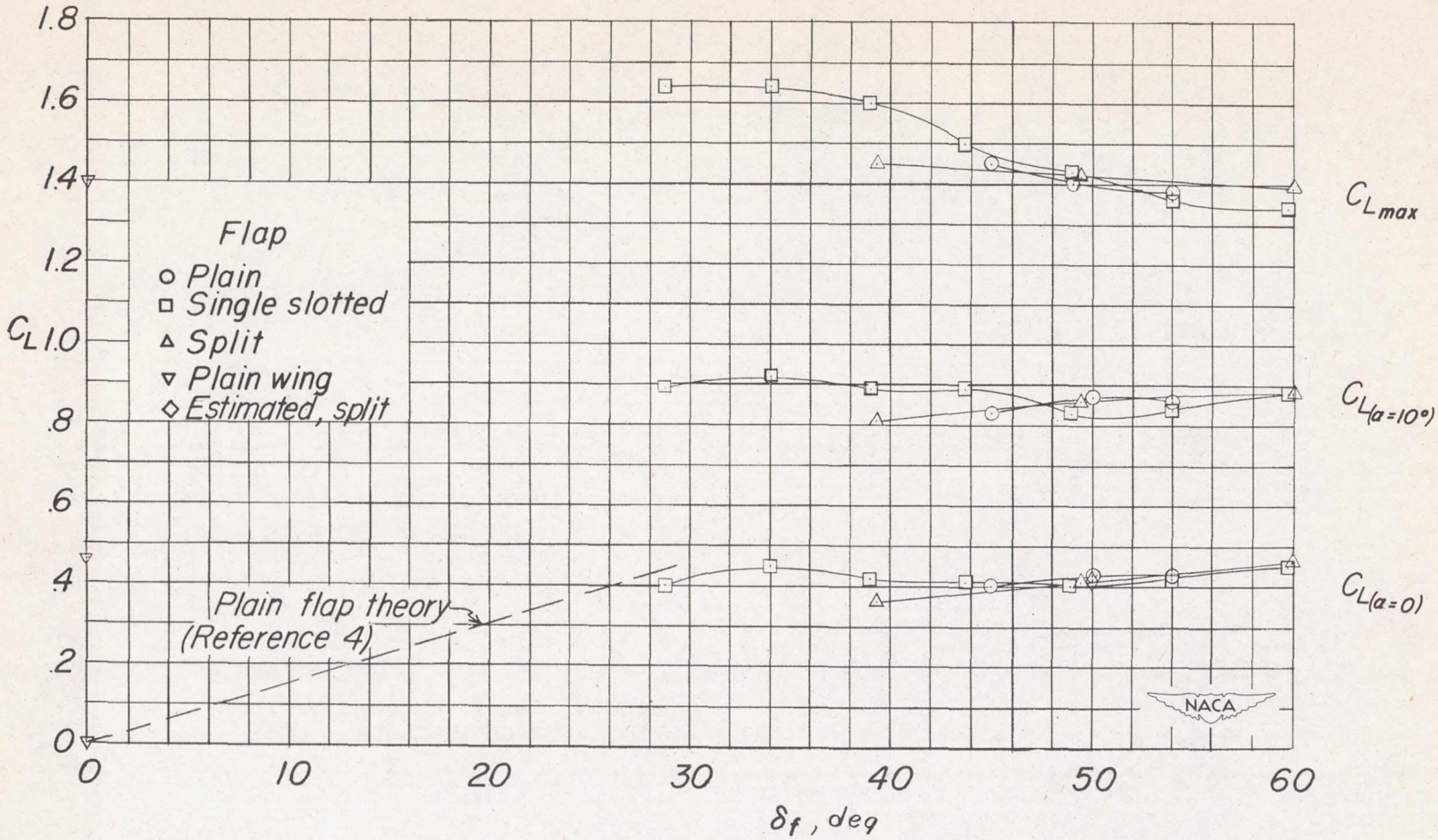

Figure 15.- The variation of C_L at $\alpha = 0°$, C_L at $\alpha = 10°$, and $C_{L_{max}}$ with deflection of the single slotted, plain, and split flaps.